4-9086

A Critical Review of the Light Scattering Technique in the Determination of Oil/Water Interfacial Tension

Energy, Mines and Resources Contract Number OST85-00053

DSS File Number 20ST.23440-4-9086

by

Dr. T. Craig

Physics Department

University of Guelph

Guelph, Ontario

N1G 2W1

December 1985.

84 pp

MICROMEDIA

This document is the final report for the contract entitled "A Critical Review of the Light Scattering Technique in the Determination of Oil/Water Interfacial Tensions" (Energy, Mines and Resources Contract Number OST85-00053, DSS File Number 20ST.23440-4-9086). Its intent was to review the literature concerning the determination of low interfacial tensions and to evaluate the feasibility of constructing a light scattering apparatus to perform this task. As well, a design for such a piece of apparatus was to be included if light scattering was found to be an appropriate technique. Given this mandate, an electronic literature review was undertaken. Including other titles found after the electronic review, approximately 90 papers concerning the determination of surface tension were found and abstracted. As well, some early works were found but not analyzed since it was thought that they would not be applicable to the present situation. Of these 90 papers some 38 were directly related to light scattering while the remainder were spread out over the various more classical techniques. It should be noted that these papers were only those which had an emphasis on the techniques themselves and not those which merely mentioned the techniques and then used them in a chemical or physical study of an appropriate system. It was found that light scattering would be a good technique to measure low surface tensions so an equipment design is included.

Table of Contents

I. Introduction 4

II. Force Measurement Methods 4
i) Wilhelmy Plate 5
ii) Sphere 6
iii) Du Noüy Ring 6

III. Meniscii Shape Techniques 8
i) Sessile Drop 8
ii) Pendant Drop 19
iii) Spinning Drop 23
iv) Flat Surface 30

IV. Miscellaneous Classical Techniques 32
i) Maximum Bubble Pressure 32
ii) Drop Weight 33
iii) Capillary 34
iv) Oscillations in an Elliptical Jet 35
v) Drainage 36
vi) Lens Measurement 38

V. Light Scattering 39
i) Classical 41
ii) Quasi-elastic 43

VI. Comparision of Light Scattering and Classical Techniques 56

VII. Description of Light Scattering Apparatus 58

VIII. Figure Captions 61

IX. Appendix I - Definition of Symbols 62

X. References 63

I. Introduction

Surfactant-brine solutions are used routinely in testiary oil recovery procedures. These micoremulsions are injected into a porous rock region and form a discontinuous brine phase with a continuous oil phase [34]. The concentration of surfactant is high enough that it is miscible with oil in all properties [65]. This solution moves through the porous rock, mixes with and displaces oil. The surfactant in this microemulsion becomes more and more dilute due to adsorption of surfactant onto the rock and injection of ground water. As the concentration of surfactant drops the mixture moves from a single phase to a multiphase region. At this point miscible displacement is replaced by immiscible displacement. The way this immiscible displacement takes place depends on interfacial tension and the anticipated oil recovery will depend on the details of the behavior in this multiphase region [37]. Of greatest interest are the areas where microemulsion-oil and microemulsion-water interfacial tensions are low and equal [37].

Since these tensions are in the region of 10^{-4} - 10^{-6} Nm^{-1} it is necessary to have extremely accurate measurement techniques. This is especially important for techniques which require optical measurements such as the Meniscii Shape Techniques which will be described in Section III.

II. Force Measurement Methods

These techniques require measurement of the force needed to detach an object from the surface of a liquid for surface tension measurements or move it from one liquid to another in the case of interfacial tension. The force reaches a maximum just before the object is detached. This force equals the apparent weight of the object added to γp where "p" is length of the

perimeter of the object. The general class of techniques known as "Detachment" or "Force Measurement" Methods were first reviewed by Adamson in 1960 [1] but are still in wide use partly because they are absolute rather than comparative techniques.

i) Wilhelmy Plate

This method involves lowering a microscope slide or thin plate into the liquid or liquids on which the analysis is to be made. This plate is connected to a sensitive balance. The liquid is gradually lowered away from the plate [1]. Perfect wetting of the plate must be assumed. This can be achieved by roughening the plate, rinsing it very thoroughly and storing it in distilled water [91]. The surface tension is given as;

$$\gamma = g\Delta m/2(\ell+t) \qquad \text{(II.1)}$$

where "ℓ" is the length of the plate, "t" is its thickness and Δm is the increment in a balance reading at the null position caused by the downward force on the plate due to the interfacial tension. This equation has no end corrections associated with it. These corrections will give an increase in γ of about 1% for a glass plate or 1.5% for a ceramic plate. For glass plates reproducibility in measurements will be ±0.1% for $\gamma > 1 mNm^{-1}$ and ±0.4% for $\gamma < 1 mNm^{-1}$ if the same plates are used. If different plates are used the errors are ±0.5% and 1% respectively. An improvement of ±0.05% can be expected for ceramic plates [91]. Two systems of interest on which this technique has been applied are toluene/water/1-propanol and toluene/sodium dodecyl sulfate/1-butanol/NaCℓ [79]. In these cases a sandblasted Teflon blade was employed. The lowest value of γ measured in this study was 2.5×10^{-4} Nm^{-1}. For lower measurements the authors used the spinning drop

technique. No complex calculations based on the shape of the meniscus surrounding the blade have been made so this method should not be taken as giving a completely accurate value of the surface or interfacial tension. It should also be noted that equation II.1 is a rather simplistic representation in that it does not explicity contain bouyancy effects.

ii) Sphere

A similar technique to i) involves lifting a sphere as opposed to a plate. Huk and Mason [39] have made detailed calculations to be used for this technique based on the shape of the meniscus surrounding the sphere. This information along with the force balance equations allows γ to be calculated. These calculations have been improved by Fieber and Sountag [28]. There are several complications associated with this technique. Firstly, relative to its volume, a sphere has a small contact line with the fluid. Thusly, a small error in the measurement of the radius creates a large error in the surface tension. Secondly, this technique involves measuring the height of the centre of mass of the sphere above the flat surface of the liquid or the flat interface between the liquids. This height can be difficult to measure. Thirdly, it is difficult to continuously measure the force required to lift the sphere. Lastly, the finite size of the container holding the liquid poses a problem. The container must be large enough that the surface of the liquid is flat but small enough that a reasonable amount of sample is used.

iii) Du Nouy Ring

In the Du Nouy Ring method a circular ring of wire is lifted from a fluid. In the simplest case equation II.1 is used with the perimeter calculated as $2(2\pi R)$. The extra factor of 2 is due to the fact that there

is an inside and outside to the ring [1]. The initial review of Adamson finds serious problems with this technique due to the correction factors that must be calculated. It does however have an experimental precision of 0.25%.

Huh and Mason [40] have improved upon the earlier works with some more complex calculations. They also give a list of references which include some much earlier works. They state that the surface tension can be calculated from;

$$\gamma = \frac{F}{4\pi R} f(R^3/V, R/a) \qquad \text{(II.2)}$$

where "R" is the radius of the ring, "a" is the radius of the wire, "V" is the maximum volume of the liquid lifted above the flat surface, and "f" is a function which equals 1 for a = 0 and R = ∞ and is called the Hawkins and Jordon factor. The factor "F" is defined as;

$$F = (\rho_1 - \rho_2)gV \qquad \text{(II.3)}$$

at mechanical equilibrium. This paper attempts to better calculate "f". There are also several problems with this method that are stated in this publication. They are; i) if the assumption that the liquid completely wets the ring is violated an error of 1% occurs for a contact angle of 10^{o}, ii) again the size of the vessel needed has to be carefully considered, iii) small errors occur due to welding a support wire to the ring, iv) it is difficult to obtain the force just as the ring leaves the fluid, and v) there can be errors due to the ring not being horizontal.

III. Meniscii Shape Techniques

The essence of the following four techniques is the accurate description of the meniscus shape between two liquids. This information then acts as input to the solution of Laplace's equation in order to determine interfacial tension. Laplace's equation describes the pressure difference across an interface in terms of the surface tension and the radii of curvature. It is given by

$$\Delta P = \gamma \left(\frac{1}{R_1} + \frac{1}{R_2} \right) \qquad \text{(III.1)}$$

where ΔP is the pressure difference across the interface and R_1 and R_2 are the two radii of curvature [2].

i) Sessile Drop

The basic experimental arrangement used for this technique is simple. A large clean glass vessel containing a liquid is placed on a levelling platform. A plane sheet of a solid substance is then placed in the vessel. Depending on the relative densities of the two liquids, the plate is either placed on the bottom of the vessel (for the drop being more dense than the other liquid) or somewhere above the bottom (for the drop being less dense than the other liquid). Using water as an example, a clean, matt surface of glass is placed on the bottom of the vessel. A small drop of a second liquid whose density is more than water and which is immiscible with water is formed on this glass surface. If the density is less, the drop is found on the underside of the glass [67]. The analysis of this drop shape provides the difficulty in the experiment and will be described below.

Figure 1 shows a slice through the meridian of a sessile drop. The drop interface in two dimensions is defined by $x = x(s)$ and $z = z(s)$ where

"s" is the arc length from the origin [81]. It is possible to reduce this to a two dimensional problem because of symmetry. R_1 is the radius of curvature in the plane of the paper and R_2 is the radius of curvature perpendicular to the plane of the paper. At the apex of the drop $R_1 = R_2 = b$. As well, some other substitutes apply

$$\cos \phi = \frac{dx}{ds} \qquad \text{(III.2)}$$

$$\sin \phi = \frac{dz}{ds} \qquad \text{(III.3)}$$

where ϕ is the angle between the tangent to the meniscii and the x-axis. By definition

$$R_1 = \frac{ds}{d\phi} \qquad \text{(III.4)}$$

and at some point (x,z)

$$R_2 = \frac{x}{\sin \phi} \qquad \text{(III.5)}$$

The pressure difference ΔP at some distance z below the surface is given by

$$\Delta P = \Delta P_o + (\Delta \rho) gz \qquad \text{(III.6)}$$

where $\Delta \rho gz$ is the term due to the hydrostatic head and $\Delta P = 2\gamma/b$. Making these substitutions into Eq. III.1 gives

$$\frac{2\gamma}{b} = \Delta \rho gz = \gamma \left(\frac{d\phi}{ds} + \frac{\sin \phi}{x} \right) \qquad \text{(III.7)}$$

From Eq. III.2 and III.3 it can be seen that

$$\tan \phi = \frac{dz}{dx} \qquad \text{(III.8)}$$

giving

$$\frac{d^2z}{dx^2} = \frac{d\phi}{dx}(\sec^2\phi)$$

$$= \frac{d\phi}{dx}(1 + \tan^2\phi) = \frac{d\phi}{dx}\left(1 + \left(\frac{dz}{dx}\right)^2\right) \qquad \text{(III.9)}$$

Now,

$$\sin\phi = \frac{dz}{dx}\frac{dx}{ds} = \frac{dz}{dx}\cos\phi \qquad \text{(III.10)}$$

However,

$$\cos\phi = \frac{1}{\sec\phi} \qquad \text{(III.11)}$$

and $$\sec^2\phi = 1 + \tan^2\phi \qquad \text{(III.12)}$$

so $$\cos\phi = \frac{1}{(1 + \tan^2\phi)^{1/2}} = \frac{1}{\left(1 + \left(\frac{dz}{dx}\right)^2\right)^{1/2}} \qquad \text{(III.13)}$$

giving $$\sin\phi = \frac{dz}{dx}\left(1 + \left(\frac{dz}{dx}\right)^2\right)^{-1/2} \qquad \text{(III.14)}$$

Substituting Eq. III.14 into Eq. III.7 gives

$$\frac{2\gamma}{b} + \Delta\rho gz = \gamma\left(\frac{d\phi}{ds} + \frac{1}{x}\frac{dz}{dx}\left(1 + \left(\frac{dz}{dx}\right)^2\right)^{-1/2}\right) \qquad \text{(III.15)}$$

As well,

$$\frac{d\phi}{ds} = \frac{d\phi}{dx}\frac{dx}{ds} = \frac{d\phi}{dx}\cos\phi \qquad \text{(III.16)}$$

Substituting Eq. III.13 and III.9 into Eq. III.16 modifies Eq. III.15 to [66],

$$\frac{2\gamma}{b} + \Delta\rho g z = \gamma\left[\frac{d^2z}{dx^2}\left(1+\left(\frac{dz}{dx}\right)^2\right)^{-3/2} + \frac{1}{x}\frac{dz}{dx}\left(1+\left(\frac{dz}{dx}\right)^2\right)^{-1/2}\right] \quad \text{(III.17)}$$

Equation III.17 provides the basis for the sessile drop technique. Solving this differential equation should yield γ for any x-z pair knowing $\Delta\rho$ and "b". It is not however possible to solve this differential equation analytically. Many techniques have been used to give results under certain circumstances.

The first attempt to solve this problem was by Bashford and Adams in 1883 [4]. They produced tables of

$$\beta = \frac{\Delta\rho g b^2}{\gamma} \quad \text{(III.18)}$$

for various values of "z" and "x". Using these tables it is possible to determine γ for a limited number of measurements of "x", "z" and the radius of curvature at the apex "b". It is not easy to determine "b" accurately however.

Another method of analyzing the shapes of sessile drops was examined in a paper by Dismukes [22]. He discusses the use of the Worthington formula;

$$\gamma = \frac{1}{2} h^2 g\Delta\rho \,/\, (1 + 0.6094\ h/r) \quad \text{(III.20)}$$

where "h" is the distance from the plane of maximum diameter of the bubble to its apex and "r" is the maximum radius of the bubble. Clearly in Eq. III.20 it is more important to be able to accurately determine "h" than "r". This means that if it is not possible to measure the coordinates of the horizontal plane of maximum diameter to better than 1.0×10^{-5}m, then for r/h = 1.03, Δh may be as large as 2.5×10^{-4}m and for r/h = 1.51, Δh may be

4.0×10^{-4}m. This indicates that for larger bubbles the relative error will be less even though the absolute error will be greater thus making it advantageous to use larger drops to get more accurate values of γ.

In 1962, Staicopolus [84] generated new tables similar to Bashford and Adams which gave values of β for particular "z"'s, "x"'s and bubble volumes. This was really the first improvement on this technique since 1883.

Significant improvements to the techniques came later in papers by Butler and Bloom [14] and Maze and Burnet [60] [59]. All of these papers used numerical methods to solve Eq. III.17 and fit it to a measurement of the half height at the maximum radius. In all cases the tables of Bashford and Adams were used as input to the programs. Program listings for the techniques are given in these papers. The great difficulty in all of these determinations is that too much weight is given to one measured point, namely the apex position. It is difficult to measure the maximum half height accurately because of the uncertainty in the measurement of that point. Maze and Burnet [59] claim that if they measure the apex to only 1.0×15^{-5}m then they generate a 5% error in γ.

The group of Padday gave three contributions to this field in the early 1970's. Firstly, in 1971 detailed computer calculations of the tables of Bashford and Adams were performed [68]. Secondly, they gave means of obtaining γ for cases of contact angles from 0 to 180° for large drops [66]. For the case of large drops $x \to \infty$ and $b \to \infty$, thus reducing Eq. III.17 to

$$\frac{d^2z}{dx^2}\left(1 + \left(\frac{dz}{dx}\right)^2\right)^{3/2} = \frac{\Delta\rho g z}{\gamma} \qquad \text{(III.21)}$$

Now substituting Eq. III.8, III.9, III.11 and III.12 yields

$$\frac{\Delta\rho g z}{\gamma} = \frac{d\phi}{dx}(\sec^2\phi)(\sec^2\phi)^{-3/2}$$

$$= \frac{d\phi}{dx}\cos\phi$$

$$= \frac{d\phi}{dz}\frac{dz}{dx}\cos\phi$$

$$= \frac{d\phi}{dz}\sin\phi \qquad \text{(III.22)}$$

Integrating Eq. III.22 from 0 to z_ϕ^∞ yields

$$\frac{\rho g z_\phi^{\infty 2}}{2\gamma} = 1 - \cos\phi \qquad \text{(III.23)}$$

Unfortunately Eq. III.23 only applies when the drop is so big as to be experimentally impractical. However, for $\phi = 90^\circ$

$$\gamma = \frac{1}{2}\Delta\rho g\,(z_{90}^\infty)^2 \qquad \text{(III.24)}$$

where z_{90}^∞ is the half height from the maximum diamter and for $\phi = 180^\circ$

$$\gamma = \frac{1}{4}\Delta\rho g\,(z_{180}^\infty)^2 \qquad \text{(III.25)}$$

where z_{180}^∞ is the full height.

Proper conditions can be obtained for $\phi = 180^\circ$. In this case the bubble actually sits on a very thin layer of the surrounding fluid. A later paper made corrections to this formalism for drops of reasonable radii [67]. A correction factor C_{180}^∞ was calculated to change Eq. III.25 to

$$\gamma = \frac{1}{4}\Delta\rho g\,(z_{180}^\infty)^2\, C_{180}^\infty \qquad \text{(III.26)}$$

They also noticed that "z" reached a maximum before it fell to its limiting value at infinite volume. In order to make correct calculations, the

product $x_{180}\,(\Delta\rho g/\gamma)^{1/2}$ must be approximately equal to 400 which for an air-water interface gives a diameter of about 2m for the bubble. They found that it was possible to measure z_{180} to ±0.002mm for any one measurement and ±0.005 mm between measurements. The following sources of error were identified by them i) a contact angle $\neq 180^{o}$ ii) thickness of the film between the drop and supporting glass not negligible iii) error in correction factor "C". They determined that if ϕ is less than 180^{o} the error in z_{180}^{∞} is proportional to cos ϕ and will produce an error in the area of 0.34% for a reasonable ϕ.

A more detailed study of the errors associated with the Padday technique was performed by Healy and Reed [34]. They showed that in the low interfacial tension regime ($\gamma \simeq 10^{-6}$ N/m), which if of particular interest in the oil-water- surfactant system a precision of about ±10% was all that could be expected using Eq. III.24 for $x_{180}/z_{180} = 5$. They added a correction factor to this equation to give

$$\gamma = \frac{1}{2}\,\Delta\rho g\,(z_{180}^{\infty})^2 \,/\, (\,1 + 0.3060\, z_{180}^{\infty}/x_{180}^{\infty})^2 \qquad \text{(III.27)}$$

which lowered the error to 2% for $x_{180}^{\infty}/z_{180}^{\infty} = 3.85$, 1% for a ratio of 4.3 and 0.5% for a ratio of 4.8. More recent measurements of this sort measured drop heights to 2%, $\Delta\rho g/2$ to 1% and overall errors of <10% for oil-water systems [23].

A better calculation of the correction factor in Eq. III.26 has been attempted by Malcolm and Elliott [56]. They modified Eq. III.26 to the form

$$\gamma = \Delta\rho g\,[z_{180}^{\infty} \,/\, G(z_{180}^{\infty}/x_{180}^{\infty})]^2 \qquad \text{(III.28)}$$

where $G(z_{180}^{\infty}/x_{180}^{\infty}) = C_1 + C_2(z_{180}^{\infty}/x_{180}^{\infty}) + C_3(z_{180}^{\infty}/x_{180}^{\infty})^2$

$$+ C_4(z_{180}^{\infty}/x_{180}^{\infty})^3 + C_5(z_{180}^{\infty}/x_{180}^{\infty})^4 \qquad \text{(III.29)}$$

This paper has extensive lists of the constants C_1 to C_4 for various shaped drops. They site the same errors as the previous authors and give approximately the same magnitudes. They claim that the error between Eq. III.28 and their data is <0.041%. They also note the fact that since this technique requires no measurement of the equator, a large source of error has been eliminated. There is one drawback however and that is that errors in z_{180}^{∞} are important since they enter the circulation as the square. In order to make the measurements such that the error in Eq. III.28 becomes unimportant z_{180}^{∞} must be measured to a precision of ±0.0006mm. At a precision of ±0.002mm, γ will have an error of 1.5%. This group has made more recent measurements with the aim of also determining contact angles [57].

The most recent paper using the method of measurement of maximum height z_{180}^{∞} was published in 1985 by Concoulas and Dawe [18]. They describe a technique to obtain the correction factor C_{180}^{∞} and define it as

$$C_{180} = \left(\frac{z_{180}^{\infty}}{z_{180}}\right)^2 \qquad \text{(III.30)}$$

where z_{180} is the maximum height for a bubble of less than infinite radius and z_{180}^{∞} is the height at infinite radius. At the maximum height C_{180}^{∞} = 0.90067 but at other heights C_{180}^{∞} can be determined from the tables of Padday [68]. They also note that it is not always possible to get

completely non-wetting surfaces for drops. In these cases it is necessary to use an interative approach as follows; i) measure x_{90}, z_ϕ and ϕ (ϕ is contact angle and x_{90} is the maximum value of the radius) ii) generate a value of β from a guess for γ iii) calculate "b" iv) read x_{90}/b and z_ϕ/b from the tables for the appropriate contact angle v) compare the ratio z_ϕ/x_{90} from the tables and compare with experiments and vi) search the tables until the experiment value of the ratio agrees with the table values. This technique is very time consuming and requires interpolation procedures which may not be accurate due to the high degree of non-linearity in the problem. They also describe a technique whereby they can reproduce the tables of Padday [68] with an analytic expression with an error of <0.05%. They describe the developement of the expression but it is only necessary to give the result here;

$$z_k = f(x_k) = 2 \sum_{i=1}^{5} C_i x_k - \frac{\sqrt{\frac{1-\cos Q}{2}}}{x_k + C_8} + C_8 \exp(0.1 C_6 x_k^{C_7}) + \frac{\sqrt{\frac{1-\cos Q}{2}}}{x_k + C_8} + C_8 \quad \text{(III.31)}$$

where $$k = \left(\frac{\gamma}{g\Delta\rho} \right)^{1/2} \quad \text{(III.32)}$$

and $$c_i = \sum_{j=0}^{6} \lambda\, a_{ij}\, T_j(\bar{Q}) \quad \lambda=0.5 \text{ for } j = 0,\ \lambda=1 \text{ for } 1<j<6 \quad \text{(III.33)}$$

$$T_n(x) = \cos(n \cos^{-1} x) \quad \text{(Tchebyshev Polynomial)} \quad \text{(III.34)}$$

and $$x_k = x_\phi/k \text{ and } z_k = z_\phi/k.$$

$\bar{\phi}$ is the normalized contact angle for the range $90 < \phi < 180$, i.e. $\bar{\phi} = -1$ at 90^o and $\phi = 1$ at 180^o. This method can only be used for

$90 < \phi < 180$ and $\beta > 0.1$. For $\beta < 0.1$ the drops are almost spherical and large errors occur in the calculation of the interfacial tension. The protocol to find γ using Eq. III.31 involves i) measuring z_ϕ, x_{90} and ϕ ii) calculating C_1 to C_8 iii) evaluating $f(x_k)/x_k$ for a random value of x_k and comparing it with the measured value of z_ϕ/x_{90}. At this point an iterative technique is used to solve the equation

$$f(x_k)/x_k = z_\phi/x_{90} \qquad \text{(III.35)}$$

for x_k. Sample data has been included in this paper so the algorithm may be programmed and the result checked. A discussion of the errors inherent in the method is also included. Flat drops give the smallest errors in γ and spherical drops the largest. Since an equation like III.25 is used to calculate γ, the percentage error in γ will be twice that in z_ϕ. It is also true that the largest errors in the determination of contact angles also occurs for spherical drops. For flat drops ($150^\circ < \phi < 180^\circ$) errors of 1° or 2° have no effect on γ. The authors reiterate that the measurement of z_ϕ is the largest source of error.

An interesting application of the height measuring technique appears in a paper by Faetti and Palleschi [27]. They measured the height of a sessile drop and related this height to the interfacial tension between the nematic and isotropic phases of some cyanobiphenyls. Their measurements had a large error in γ of about 10%.

Most of the papers on sessile drops in the 1980's have involved either improvements in the measurement of meniscii shapes [31][55][75] or improved methods of fitting meniscii shapes to Laplace's equation [81][41][13]. Of the new measurement techniques, Los et al. [55] use a novel illumination

procedure to best view the drop profile, Girault et al. [31] use a 128 x 128 pixel image of a drop with 8 bit resolution to fit to Laplace's equation and Qutubuddin et al. [75] have computerized data acquisition using a digitizing system. This last group have used their system in the low interfacial tension regime for a n-decane:oleic acid:2-pentanol:brine mixture. Oleic acid and 2-pentanol are the surfactant and cosurfactant respectively in this sample.

The first paper to shown an improved method of data fitting appeared in 1983 [81] by Rotenberg et al. They simply found the minimum of

$$E = \frac{1}{2} \sum_{n=1}^{N} [d\ (u_n,\ v)]^2 \qquad \text{(III.36)}$$

where $d(u_n,v)$ is the perpendicular distance between the measured data points "u_n"'s and "v" the Laplace curve solved by numerical methods. There are "N" data points in the sample from a suitable medium (video or digitized film). The software to perform this fit may be purchased from the authors. A second paper appeared in 1983 concerning the fitting of meniscii shapes [41]. It is very similar to the previous paper but not so well thought out and complete. The Rotenberg group published and improved their work one year later [13]. They used as a sample system a mixture of sodium dodecyl sulfate in one phase and a combination of cholesterol in dibutyl phthalate mixed 1:1 with diatyl phthalate in the other phase. Ten measurements on this system yielded $\gamma = 5.783 \pm 0.201 \times 10^{-3}$ mN m^{-1} which is a standard error of ± 3.4%. They estimated the digitizing error as ± 0.2% on about 40 points. The error actually becomes less as γ gets smaller. It is also stated in this paper that the sessile drop method is faster and better than

the pendant drop method for low γ. Unlike the method of Huh and Reed [41] it is not necessary to enter x_ϕ and z_ϕ which adds another source of error. As well, unlike Huh and Reed, they use the perpendicular distances between the theoretical and measured curves. Using these perpendicular distances between the data and Laplace's equation lowers the effects of the positioning of the apex. Rotenberg's method also is useful for both pendant and sessile drops and for $\phi < 90^o$.

ii) Pendant Drop

Again, as in the case of the sessile drop the experimental setup is conceptually simple. A drop of liquid is simply allowed to hang from the tip of a capillary into another liquid. The shape of the drop is then analyzed and the surface tension determined using Laplace's equation. A diagram of the geometry of the pendant drop is shown in Figure 2.

The method of solution of the problem of solving Laplace's equation is simply one of force balance. With respect to Figure 2, it can be seen that

$$F_1 + F_3 = F_{2z} \qquad \text{(III.37)}$$

where F_1 is the apparent weight of the drop under plane P, F_{2z} is the vertical projection of the tension which acts parallel to the interface at plane P and F_3 is the vertical component of excess pressure due to the interface curvature [2] [30]. From Laplace's equation

$$F_3 = \Delta P \text{ Area}$$

$$= \gamma \left(\frac{1}{R_1} + \frac{1}{R_2} \right) \pi x^2 \qquad \text{(III.38)}$$

where R_1 and R_2 are the radii of curvature as before and "x" is the cross-

sectional radius at plane P. Now

$$F_1 = \Delta\rho g V \tag{III.39}$$

where V is the volume of the drop below plane P and

$$F_{2z} = 2\pi x\gamma \sin\phi \tag{III.40}$$

Combining Eq. III.37, III.38, III.39 and III.40 gives

$$V\Delta\rho g + \gamma\left(\frac{1}{R_1} - \frac{1}{R_2}\right)\pi z^2 = 2\pi x\gamma \sin\phi \tag{III.41}$$

The same substitutions that gave Eq. III.17 from Eq. III.1 can be invoked for Eq. III.41 as well, giving

$$\frac{d^2z}{dx^2} + \frac{1}{x}\frac{dz}{dx}\left[1+\left(\frac{dz}{dx}\right)^2\right] = \left[2-\beta z\right]\left[1+\left(\frac{dz}{dx}\right)^2\right]^{3/2} \tag{III.42}$$

where "V" is volume below this plane.

In the initial paper by Andreas et al. using this technique some simplifying assumptions were made [2]. The first involved choosing the plane P such that it was at the point of inflection of the meniscus, i.e. where $\frac{1}{R_1} = o$ and $R_2 = \frac{x}{\sin\phi}$. This eliminated the problem of measuring R_1. Thus simplifying III.42 to

$$\gamma = \frac{V_{inf}\ \Delta\rho g}{\pi\ X_{inf}\ \sin\phi_{inf}} \tag{III.43}$$

Two problems were associated with this, namely; i) it is difficult to determine the point of inflection and ii) the volume of the drop below the plane can not be accurately determined from the profile.

The second simplified case required the choosing of a second plane

other than the equator, of diameter d_s. The equator diameter is d_e and the ratio "S" is defined as

$$S = \frac{d_s}{d_e} \qquad \text{(III.44)}$$

As well, "H" is defined as

$$H = \beta \left(\frac{d_e}{b} \right)^2 \qquad \text{(III.45)}$$

and

$$\gamma = \frac{g\Delta\rho(d_e)^2}{H} \qquad \text{(III.46)}$$

Tables of S vs 1/H were calculated so that γ could be determined. These tables were later extended by Stauffer [85] who also stated that just as in the case of sessile drops, spherical pendant drops give the largest errors. Andreas et al. also listed a set of advantages of this technique (these also apply to the sessile drop) some of which are still applicable, i) a complete mathematical analysis is available ii) it is independent of contact angle iii) no viscosity effects need to be taken into account iv) measurements can be instantaneous v) successive measurements can be made vi) interfacial tensions in the range 0.4 Nm^{-1} to 3.0 x 10^{-4} Nm^{-1} can be measured vii) any two fluids can be used if one is transparent viii) only small samples are needed ix) temperature control is possible and x) the photos taken of the profiles are permanent records.

Other authors have used the selected plane method to determine γ. Michaels and Hauser [62] studied benzene:water, benzene:air, n-decane: air interfaces. They determined that these systems were difficult since it was hard to determine $\Delta\rho$ accurately because the liquids were so nearly equal in density.

More recently, it has been pointed out that a method based on hydrostatic equilibrium between the apex of the drop and the plane P gives results equivalent to Eq. III.41 [30]. In the hydrostatic technique

$$\Delta P = P_{PLANE} - P_{APEX} = g\Delta\rho z \qquad \text{(III.47)}$$

so giving

$$\gamma \left[\frac{1}{R_1} + \frac{1}{R_2} - \frac{2}{b} \right] = g\Delta\rho z \qquad \text{(III.48)}$$

which is identical to Eq. III.41 if "V" is determined from

$$V = \int_{APEX}^{y} \pi x^2 dz \qquad \text{(III.49)}$$

These authors have also applied the inflexion point approach to the problem but due to the advent of computers have avoided the two problems of Andreas et al. They also give a list of advantages of the sessile and pendant drop techniques for measurement of interfacial tension i) both are absolute and ii) equilibrium techniques iii) the experimental setup is trivial and iv) they lend themselves to automation and computer analysis.

Many of the publications presented previously in the sessile drop section have applications to pendant drops as well [68], [55], [81], [41] and [13]. Also another paper is presented in the literature which is simply an application of the Butler and Bloom [14] technique for sessile drops to pendant drops [71]. It is of special interest since it points out some of the pitfalls with this method of interfacial tension determination namely; i) a low vibration system must be used ii) temperature control must be rigorous and iii) photos must be taken on glass plates as opposed to paper to avoid differential shrinkage. They also quote standard deviations on

the measurement of the surface tension of water of 0.22% and on the interfacial tension between water and benzene of 0.35%.

iii) Spinning Drop

Two of the initial publications on this technique were published in 1962 by Rosenthal [80] and in 1967 by Princen et al. [73]. They both describe a method whereby a drop of one fluid is placed in a horizontal tube filled with another fluid and subsequently spun about its long axis. The drop forms an elongated structure symmetric about the axis of rotation. The shape of this structure is determined by γ and the rotational frequency ω, through Laplace's equation. A block diagram of a modern spinning drop apparatus as taken from a paper by Cayias et al [15] is shown in Figure 3. Figure 4 shows the geometry of the spinning drop formed. Note that ϕ is the angle between the normal to the interface and the negative z direction.

The essence of the technique is described fully in the two previously mentioned papers. What follows is more directly from Princen et al. [73] since it more closely resembles the formalism for the sessile end pendant drop. A drop, density ρ_1, is spun in a horizontal tube filled with a fluid of density ρ_2. The pressure outside the drop is defined as

$$P_2 = P_o + \frac{\rho_2 \omega^2 x^2}{2} \qquad \text{(III.48)}$$

while inside it is

$$P_1 = P_o + \frac{\rho_1 \omega^2 x^2}{2} + \frac{2\gamma}{b} \qquad \text{(III.49)}$$

At the surface of the bubble the pressure difference is

$$\Delta P = P_1 - P_2 = \frac{2\gamma}{b} + \frac{\Delta\rho\omega^2 x^2}{2} \qquad \text{(III.50)}$$

This pressure difference is balanced by the capillary pressure described by Laplace's equation, to yield

$$\frac{2\gamma}{b} + \frac{\Delta\rho\omega^2 x^2}{2} = \gamma \left(\frac{1}{R_1} + \frac{1}{R_2} \right) \qquad \text{(III.51)}$$

Princen makes the substitutions

$$\frac{1}{R_1} = \frac{d \sin \phi}{dx} \qquad \text{(III.52)}$$

and

$$\frac{1}{R_2} = \frac{\sin \phi}{x} \qquad \text{(III.53)}$$

to give

$$\frac{d \sin \phi}{dx} + \frac{\sin \phi}{x} = \frac{2}{b} - \frac{\Delta\rho\omega^2 x^2}{2\gamma} \qquad \text{(III.54)}$$

or

$$\frac{d \sin \phi}{dX} + \frac{\sin \phi}{X} = 2 - \alpha X^2 \qquad \text{(III.55)}$$

where $X = x/a$ and

$$\alpha = \frac{\Delta\rho\omega^2 b^3}{2\gamma} \qquad \text{(III.56)}$$

Thus the shape is determined by α. Now Eq. III.55 can be integrated to give

$$\sin \phi = X \left(1 - \frac{2X^2}{4} \right) \qquad \text{(III.57)}$$

There are three simplifications that can be made at this stage. Firstly, at

the maximum diameter of the bubble x_o, sin ϕ = 1 and

$$\alpha X_o^3 - 4X + 4 = 0 \qquad \text{(III.58)}$$

The roots of this equation give X_o as a function of α so γ may be determined if b, ω and $\Delta\rho$ are known.

The second simplification that can be performed involves differentiating Eq. III.57 to give

$$d \sin \phi = \left(1 - \frac{3\alpha X^2}{4} \right) dX \qquad \text{(III.59)}$$

then multiplying the left side by tan ϕ, the right side by $\frac{dZ}{dX}$ and integrating from o,o to X_o,Z_o.

This gives

$$1 = Z_o - \frac{3\alpha}{4} \int_o^{Z_o} X^2 \, dZ \qquad \text{(III.60)}$$

However $$\frac{V}{b^3} = 2\pi \int_o^{Z_o} X^2 \, dZ \qquad \text{(III.61)}$$

which gives $$\frac{V}{b^3} = \frac{4\pi}{3} \left(\frac{r}{a} \right)^3 = \frac{8\pi}{3\alpha} (Z_o - 1) \qquad \text{(III.62)}$$

or $$\frac{r}{a} = \left[2\left(\frac{Z_o - 1}{\alpha}\right) \right]^{1/3} \qquad \text{(III.63)}$$

where "r" is the radius of a sphere of the same volume as the drop.

The last simplification occurs at the limiting case of high ω. At this point the drop is a cylinder will rounded ends $\phi = 90^o$, $\frac{d \sin \phi}{dX} = 0$, $X = X_o$ and

$$\alpha X_o^3 - 2X_o + 1 = 0 \qquad \text{(III.64)}$$

This only gives a one positive real result for $\alpha = 16/27$ which gives $X = 3/2$ in the limiting case and

$$\alpha = \frac{\Delta\rho\omega^2 x_o}{4} \qquad \text{(III.65)}$$

Solutions for $0 < \alpha < 16/27$ are developed in the paper but are too complex to be presented here.

Princen et al. also give three other equations that apply for large ω which allow the calculation of γ with measurement of the length and the volume of the drop, namely;

$$Z_o = Cr^3 + 1 \qquad \text{(III.66)}$$

$$r/b = \frac{3}{2}(Cr^3)^{1/3} \qquad \text{(III.67)}$$

and

$$\frac{Z_o}{X_o} = \frac{2}{3}(Cr^3 + 1) \qquad \text{(III.68)}$$

where $C = \alpha/2b^3$. These equations show that it is essential to measure ω and V correctly since $\gamma \alpha \omega^3 V^n$ where $n > 3/2$. In principle it is possible to obtain γ without knowing "V", since from Eq's III.65, III.66 and the definition of α one obtains

$$G\left(\frac{1}{\gamma}\right)^{1/3} = H\left(\frac{r^3}{\gamma}\right) + 1 \qquad \text{(III.69)}$$

where

$$G = \frac{3X_o}{2}\left(\frac{\Delta\rho\omega^2}{4}\right)^{1/2} \qquad \text{(III.70)}$$

and

$$H = \frac{\Delta\rho\omega^2}{4} \qquad \text{(III.71)}$$

If the length is measured for two or more speeds giving G_1, G_2, H_1 and H_2 so

$$\gamma = \left(G_1 - H_1 \left(\frac{G_1 - G_2}{H_1 - H_2} \right) \right)^3 \qquad \text{(III.72)}$$

This has problems associated with it though since $G_1 (H_1-H_2)/H_1 (G_1-G_2)$ is never much greater than unity so a small error in ω creates a large error in γ. It is of interest that viscosity plays no role in these measurements. One possible source of error however occurs since the ω of the drop may not be the same for ω for the cylinder due to buoyancy effects. These effects are small at high ω.

A slightly different approach to the problem was proposed by Patterson et al. (BX). Using the forms of Eq. III.66 and III.67 and by knowing that

$$\gamma = \frac{\Delta\rho\omega^2}{4C} \qquad \text{(III.73)}$$

they constructed a table of "C" for various combinations of z_o and "r" to determine γ. They applied these techniques to polymer systems.

A more recent treatment of the method (Cayias et al. [15]) has elucidated the errors that are involved. They state that the ratio of the length to the width must be greater than 3.5 in order to apply either Eq. III.65 or III.72 to the problem, that is, measure only x_o or z_o to determine γ. They also noted that the axis of rotation must be very carefully aligned horizontally. The experimental technique is described fully in this publication with careful attention paid to the tube loading. They fill the tube completely with the more dense phase, hold the tube upside down and inject the lighter phase up into it using a syringe. They claim a precision of 10% for low surface tension systems and state that it is

possible to measure to $10^{-6}Nm^{-1}$ with good optics. Good optics are essential to obtaining accurate measurements. Drop break-up is another major problem associated with this technique according to these authors and the experiment must be terminated if this occurs.

A detailed study was performed some eight years ago using the University of Texas Interfacial Spinning Drop Tensiometer [58]. These authors were interested in making measurements to the fractions of percent level. They state that i) it is necessary to have ω high enough so that gravity may be ignored and ii) if care is not taken secondary flows can be set-up which will tend to break up the drop. These flows can be caused by gravity if the rotational axis is not horizontal or by vibrations in drives and bearings. The simplest way to determine if equilibrium has been reached is to get a constant value for the product $\omega^2 x_o^3$. This must be done in any case to validate the results. As well, they give the definitions for the following parameters and use them to design an appropriate instrument.

$$\text{Bond Number} \equiv \frac{\omega^2 x_o^3 \Delta\rho}{\gamma} = \frac{\text{centrifugal buoyancy force}}{\text{interfacial tension force}} \qquad \text{(III.74)}$$

$$\text{Froude Number} \equiv \frac{\omega^2 x_o}{g} = \frac{\text{centripetal acceleration}}{\text{gravitational acceleration}} \qquad \text{(III.75)}$$

$$\text{Reynold's Number} \equiv \frac{\omega x_o^2}{r} = \frac{\text{inertial force}}{\text{viscous force}} \qquad \text{(III.76)}$$

$$\text{Frequency Ratio} \equiv \frac{\omega_o}{\omega} = \frac{\text{disturbance frequency}}{\text{rotational frequency}} \qquad \text{(III.77)}$$

$$\text{Rossby Number} \equiv \frac{u}{\omega R} = \frac{\text{convective acceleration}}{\text{coriolis acceleration}} \qquad \text{(III.78)}$$

To design a good instrument the Froude Number should be large, the Rossby and Reynold's Numbers and frequency ratio small and the Bond Number small compared to the Reynold's Number. To achieve this they give special emphasis to the tube used to house the fluids. It should be large enough to accomodate the initial drop without having excessive wall contact but should be small enough to increase viscosity effects to damp out unwanted vibrations. Different sized tubes are necessary for different fluids and good bearings on the drive are absolutely essential.

Experiments performed on oil:surfactant:brine systems by Puig et al. [24] show the care which must be taken when using this apparatus. They used two surfactants; i) sodium p(1-heptylmonyl) benzene sulfonate and ii) petroleum sulfonate Petronate TRS 10-80 in n-decane: brine systems. The densities of the components were measured to a precision of 20×10^{-3} kg/m^3, the index of refraction of the aqueous phase was measured to 0.0002 in order to correctly get the optical magnification factor and the drops were left spinning so there was no change in shape for 12 hours. These systems formed a disperse liquid crystalline phase when the solubility of the surfactant is exceeded. The size distribution of units in this region was found to depend on the order of mixing. These authors also describe in some detail the phase behavior in this system. This same group in a more recent paper has described even more completely the care that must be taken in order to perform accurate spinning drop measurements [83]. They use precision glass tubing for sample holders so that the drop diameters may be measured without stroboscopic illumination. Air bearings are used on the drive to avoid heating and mechanical vibration. The drive used was variable in speed up to 15×10^3 r.p.m. with a speed stability of better than 0.3%. They were

also able to measure the apparent drop diameter to better than 10^{-7}m. It is also stated in this paper that eccentricities of $2 - 3 \times 10^{-5}$m in the precision glass tubing will cause errors of 0.5% in the measurement of the apparent drop diameter. In some cases the drop may shift up to 30% away from the axis of rotation once per revolution. This requires stroboscopic illumination to correctly measure the diameter. Due to the fact that the glass tubing acts like a lens, the magnification factor must be calculated. It is however simply equal to the relative index of refraction, n, of the heavier liquid with respect to air. This gives $x_o = x_{o,\ apparent}/n$. Paralax error in the measurement of the diameter can be as high as 1% for a drop as large as 3.0×10^{-3}m but is as small as 0.1% for low surface tension systems. The compounding of all these errors including an error of 1×10^{-1} kg/m^3 for the densities of the liquids gives an overall error in the measurement of γ using Eq. III.65 of 0.1% if the length of the drop is not less than 5 times its diameter. Generally, it is best to use the lowest speed of rotation that will give gyrostatic equilibrium since $(x_{o,\ apparent})$ is proportional to $\omega^{-2/3}$ so the diameter is large thus giving better measurements. For a γ of 1×10^{-5} Nm^{-1} ω should be $5 - 6 \times 10^3$ r.p.m. Having said all of the above, they also state that in the low surface tension regime an error of 2% or more can be expected. This same group has recently published a paper determining interfacial tensions when three phases are present [82].

iv) Flat Surface

Of the techniques available to determine surface tension or interfacial tensions by the description of meniscii shapes, the flat meniscus method is conceptually the simplest. The fluid or fluids are simply placed in a

rectangular glass container large enough so that the walls are considered to be independent. This is shown diagramatically in Figure 5. Again Laplace's equation is used to solve the problem. The simplification that $R_2 = \infty$ can be made however. This is true since the curvature in the z-y plane equals zero. This reduces Laplace's equation to

$$\frac{2z}{a^2} = \gamma \frac{d^2z}{dx^2} \left(1 + \left(\frac{dz}{dx} \right)^2 \right)^{-3/2} \qquad \text{(III.79)}$$

where "a" is the capillary length defined as

$$a = \left(\frac{2\gamma}{\Delta\rho g} \right)^{1/2} \qquad \text{(III.80)}$$

Integrating this and setting $dz/dx = o$ and $z = o$ gives

$$\frac{z^2}{a^2} = 1 - \left(1 + \left(\frac{dz}{dx} \right)^2 \right)^{-1/2} \qquad \text{(III.81)}$$

Integrating a second time gives

$$x = \left(\frac{a}{\sqrt{2}} \right) \cosh^{-1} \left(\frac{\sqrt{2}a}{z} \right) - a \left(2 - \frac{z^2}{a^2} \right)^{1/2} + x_o \qquad \text{(III.82)}$$

The boundary conditions are

$$\frac{dz}{dx} = -\cot \phi \text{ at } x = o \qquad \text{(III.83)}$$

and $$z = a (1 - \sin \phi)^{1/2} \text{ at } x = o \qquad \text{(III.84)}$$

It is not possible to measure the contact angle since it is so small. Some assumptions must be made, namely;

$$z^2/a^2 \ll 1 \qquad \text{(III.85)}$$

$$\left(2 - \frac{z^2}{a^2} \right)^{1/2} = \sqrt{2} \qquad \text{(III.86)}$$

and $$\cosh u = \frac{e^u}{2} \qquad \text{(III.87)}$$

where $$u = \frac{\sqrt{2}\,(x + \sqrt{2}\,a - x_o)}{a} \qquad \text{(III.88)}$$

This reduces Eq. III.82 to

$$z = 2\sqrt{2}\,a \exp\left(-\sqrt{2}\,\frac{(a\sqrt{2}-x_o)}{a} \right) \exp\left(\frac{-\sqrt{2}x}{a} \right) \qquad \text{(III.89)}$$

The errors resulting from all of these assumptions are less than 5%.

The experimental procedure is to measure the exponential profile and determine the characteristic length $a/\sqrt{2}$. Measurements are taken far enough from the cell wall so the contact angle may be neglected. The measurements are made from photographs of the meniscus. Great care must be taken to align the photographic apparatus. The error in measurement is mainly due to the clarity of the image with standard deviation in multiple measurements is about 5%.

IV Miscellaneous Classical Techniques

i) Maximum Bubble Pressure

In this technique bubbles of one liquid are blown from the end of a small tube submersed in another [1]. It can be shown that the maximum pressure when the bubbles are blown out occurs if the they are hemispherical. The experiment then is to measure the maximum gas pressure in the tube as bubbles grow and break away. The appropriate equations then

are

$$\Delta P_{max} = (P_{max} - P_H) \qquad \text{(IV.1)}$$

where ΔP_{max} is the pressure head at the point at which the tube is under the liquid, P_{max} is the measured pressure and

$$\Delta P_{max} = \frac{2\gamma}{r} \qquad \text{(IV.2)}$$

where "r" is the radius of the tube. These equations apply for $r/a < 0.05$ where "a" is the capillary constant. The author gives a more accurate equation to be used in the analysis, namely;

$$a^2 = hr \left(1 - \frac{2r}{3h} - \frac{r^2}{6h^2} \right) \qquad \text{(IV.3)}$$

where $h = a^2/b + z$, "b" is the radius of curvature at the apex of the bubble and "z" is the distance from the fluid surface to the apex. With appropriate rearrangements this equation can be used along with the tables of Bashford and Adams to determine γ. Adams claims an accuracy of a few tenth's of a percent. These measurements can be made rapidly and they use freshly formed interfaces. This technique does not lend itself to liquid-liquid tensions but is of use for liquid-gas tensions.

ii) Drop Weight

This method consists of allowing drops of a liquid to fall from the end of a tube submerged in another liquid [1]. The weight of each drop is related to γ through

$$W = 2\pi r\gamma \qquad \text{(IV.4)}$$

Actually some reduced weight W' is measured due to the details of drop

production. It is necessary to determine the details of the size of critical drops and the precise value of W′. Tables of corrections are given by Adams [1]. This technique performs well in the case of liquid-liquid interfaces. In this case W′ is the weight less the weight of fluid displaced.

This technique has been applied recently to oil/dispersant systems (W). In this case the reduced surface tension that a surfactant gives lowers the energy required to increase the oil's surface area by the formation of small droplets. These authors give detailed drawings of their apparatus which will not be included here. They measure the effectiveness of their surfactant by determining the drop weight as a function of its concentration.

iii) Capillary

This method is extremely simple. The height of capillary rise of a liquid in a tube filled with another liquid is related to the interfacial tension by

$$\frac{a^2r^2}{2R} = \frac{r^2(h+R)}{2} + \frac{(R^2-r^2)^{2/3}}{3} - \frac{R^3}{3} \qquad \text{(IV.5)}$$

where "a" is the capillary constant, "h" is the measured rise and "R" is the radius of curvature of the meniscus [1]. Now cos ϕ = r/R where ϕ is the contact angle. The most useful and accurate form of this equation is for the case when ϕ = o. Corrections to Eq. IV.5 must be given for large capillaries where the meniscus is not hemispherical. This technique is very well understood and the experimental parameters can be well controlled. The only possible problems are with the capillary itself. It must be of circular cross-section and must be accurately vertical. This technique can

be one of the best and most accurate but large volumes of samples are needed and for maximum accuracy it is important to have a zero contact angle.

Wims et al. [92] used a modification of this technique to measure the interfacial tension between 3-methylpentane and nitroethane. They put these two liquids in a container and in this container put two capillaries. The difference in height of the interfaces in the two tubes is related to the interfacial tension by;

$$a^2 = \Delta h \, (b_1^{-1} - b_2^{-1})^{-1} \qquad \text{(IV.6)}$$

where "a" is the capillary constant, Δh is the difference in heights of the bottoms of the two meniscii and the "b"'s are the radii of curvature of the menscii where the two principle radii are equal. The capillary rise must be corrected for the amount of fluid above the bottom of the meniscus. A tabular method followed by interpolation allows the determination of "a^2" from "Δh".

iv) Oscillating Elliptical Jet

This obscure technique is only useful for measuring surface tensions and involves forcing a jet of fluid through an elliptical orifice [1]. This jet is unstable and oscillates about the preferred circular cross-section. For the case of an "ideal" jet which only has 2-dimensional oscillations

$$\gamma = \left[\frac{1}{t^2} (\rho r)^{2/3} \left(\frac{f}{\lambda} \right)^2 \right]^{2/5} \qquad \text{(IV.7)}$$

where "t" is the period of the oscillations, λ is the wavelength, "f" is the flow rate and "r" is the radius of the jet where its cross-section is circular. The orifice must have a high degree of ellipticity. There are

however enormous complications associated with this technique which reduce its precision.

v) Drainage

A series of papers by Baird and Nirdosh [3] and Ranna Rao and Baird [76] [77] have described a series of techniques known as drainage methods. These involve a bubble of either gas or liquids moving in either i) vertical tapered tubes ii) rotating uniform tubes or iii) tilted uniform tubes. A diagram of the vertical tapered tube apparatus is shown in Figure 6. The height "y" that a bubble or droplet rises in such an apparatus is related to γ by

$$\frac{\Delta\rho g d^2}{\gamma} = E_o \qquad \text{(IV.8)}$$

where "d" is the diameter of the tube at the top of the bubble, and E_o is the Eötvös or Goucher number and has a value of 5.37. This number contains all the details of the drainage mechanism around the bubble. The diameter "d" is obviously related to "y", the height of rise.

The experimental method involves cleaning the glassware extremely well, filling the tube by the stopcock and then injecting the bubble from the bottom. They claim measurements with accuracy of 0.1% can be made.

More accurate measurements can be made if the rate of climb of the bubble or drop is measured [3]. This rate is determined by how fast the more dense phase can drain around the drop or bubble through an annular ring of thickness.

$$\delta = C(d - d_o)2 \qquad \text{(IV.9)}$$

where d_o is the critical diameter which prevents the bubble from rising and

"C" is a constant. The rate of laminar drainage is then given by

$$Q = \frac{\Delta\rho g\, \delta^3 (\pi d_o)}{3\mu} \qquad \text{(IV.10)}$$

where μ is the viscosity of the dense phase. By continuity, from the velocity of the nose of the bubble,

$$Q = \frac{\pi d_o^2}{4} \frac{dy}{dt} \qquad \text{(IV.11)}$$

Equating Eq. IV.10 and IV.11 gives

$$\frac{dy}{dt} = \frac{\Delta\rho g\, C^3}{6\mu d_o} \qquad \text{(IV.12)}$$

setting $d_o = d_1 - \beta y_o$ with β being the tube taper yields

$$\frac{dy}{dt} = \frac{\Delta\rho g\, \beta^3 C^3}{6\mu d_o} (y_o - y)^3 \qquad \text{(IV.13)}$$

Integrating Eq. IV.13 gives

$$\frac{1}{(y_o - y)^2} = \frac{\Delta\rho g\, \beta^3\, C^3}{3\mu d_o} + \text{constant} \qquad \text{(IV.14)}$$

The constant is set equal to zero since at t=o the bubble is far from equilibrium. Plotting y vs $t^{-1/2}$, y_o and "C" can be obtained thus yielding a precise value of γ from Eq. IV.9 and IV.8. An assumption used in this method is that E_o is constant for a given taper. One other problem with this technique is tht E_o was calculated for a straight tube so some corrections should be made for a tapered tube.

A modification of this technique is to ulitize a tilted straight tube.

In the case $g' = g \cos \theta$ where θ is the angle of tilt must be substituted into Eq. IV.8. The measurements can then be made much as before. A further change is to spin a tube resting horizontally. A tube with stopcocks at either end and in the centre is spin about its centre. The liquid drop is then injected into the tube at each end. After about 20 minutes spinning the distances that the drops are from each end are averaged and used to determine γ from Eq. IV.8. The acceleration due to gravity is replaced by the angular acceleration at the position of the drop $\omega^2 R$. It is also necessary to modify E_o for use with this technique. By calibration by the authors it was found that

$$E_o' = 3.235 - \frac{3.424g}{\omega^2 R} + \frac{2.24g^2}{\omega^4 R^2} - \frac{0.54g^3}{\omega^6 R^3} \qquad \text{(IV.15)}$$

was more appropriate.

One of the later papers by these authors [76] performs more detailed calculations for the Eötvös number taking into account the proper drainage around the meniscus. The most recent paper by them [77] describes a method whereby continuous measurement of γ can be performed. It is not of much use although it does give the proviso for the technique in general, that is, they state that drainage methods are of little use for surfactant systems due to the large amount of time needed for equilibrium to be reached.

vi) Lens Measurement

The last technique in the classical methods section is one which was developed to look at interfacial tensions in lipid bilayers [64]. Here a lens of bulk lipid was injected into a black lipid membrane. The edges of this lens can be easily viewed and photographed. This lens has a known volume V and forms two essentially spherical segments. V is related to the

thickness "d" and base radius "r′" of the lens by

$$V = \frac{\pi}{3}(3dr'^2 + d^3) \qquad \text{(IV.16)}$$

From Eq. IV.16 "d" can be determined by measuring "r′". Knowing the lens height and base radius the radius of curvature "R" can be calculated and the contact angle ϕ is given by

$$\sin \phi = \frac{r'}{R} \qquad \text{(IV.17)}$$

and the membrane-lens interfacial tension is given by

$$\sigma = 2\gamma \cos \phi \qquad \text{(IV.18)}$$

where γ is the equilibrium value of the membrane tension. The experimental setup is very complicated for these measurements and it seems of limited usefulness.

V. Light Scattering

Light scattering techniques for the determination of interfacial and surface tension, both classical (static) and quasi-elastic, rely on the scattering of light by oscillations thermally excited on the surface of a liquid or on the interface between two liquids. These waves may be of two types i) fluctuations in vertical positions of molecules (which cause light scattering) and ii) in-plane longitudinal and shear waves (which are not coupled to light scattering) [52]. The first type of oscillations are known as thermal ripplons and have an amplitude of ~ 0.5 nm. They are characterized by a wave vector $\vec{q}$ related to their wavelength Λ by:

$$|\vec{q}| = \frac{2\pi}{\Lambda} \qquad (V.1)$$

For scattering to take place this wave vector must equal the scattering vector in the plane of the surface. The geometry for this situation is shown in Figure 7. The x-y plane is the plane of the interface. The wave vector of the incident radiation, $\vec{k}_o$, and of the reflected radiation, $\vec{k}_r$, are chosen to be in the z-y plane with $\vec{k}_o$ and $\vec{k}_r$ both making an angle θ with the positive z-axis. The scattered wave vector, $\vec{k}_s$, makes an angle θ_o with the positive z-axis and an angle Δ with the positive y-axis. The scattering vector $\vec{K}$ for thermal ripplons therefore is defined as

$$\vec{K} = \vec{k}_s' - \vec{k}_r' \qquad (V.2)$$

where $\vec{k}_s'$ and $\vec{k}_r'$ are defined as the projections of the scattered and reflected wave vectors on the surface plane [53]. The components of these vectors are [49]

$$k_{rx}' = 0 \qquad (V.3a)$$

$$k_{ry}' = k_r' \sin\theta \qquad (V.3b)$$

$$k_{sx}' = k_s' \sin\theta_o \sin\Delta \qquad (V.3c)$$

$$k_{sy}' = k_s' \sin\theta_o \cos\Delta \qquad (V.3d)$$

giving

$$|\vec{K}|^2 = K_x^2 + K_y^2$$

$$= (k_{sx}' - k_{rx}')^2 + (k_{sy}' - k_{ry}')^2$$

$$= k^2 (\sin^2\phi_o + \sin^2\phi - 2 \sin\phi \sin\phi_o \cos\Delta) \quad (V.4)$$

since $k_o = k_s' = k_r' = k$.

i) Classical

The ripplons on the surface or interface are described by

$$\xi = \xi_o e^{-\alpha t} e^{-iqx} \quad (V.5)$$

where $\alpha = i\omega_o - \Gamma$. The frequency, ω_o, of these waves is determined by the surface tension γ while the damping rate, Γ, is determined by the shear viscosity η [24]. The change in energy per unit area caused by these ripplons involves the work done in increasing the interface surface area [24];

$$\Delta E = \frac{1}{4} \xi^2 [\gamma q^2 + \Delta\rho g] \quad (V.6)$$

This gives a mean square amplitude for the fluctuations of

$$< |\xi|^2 | = \frac{k_B T}{\gamma q^2 + \Delta\rho g} \quad (V.7)$$

where k_B is Boltzman's constant and T is the absolute temperature and $\Delta\rho$ is the difference in densities between the two fluids for an interface or just the density of the liquid for a surface. Now the mean squre amplitude of the fluctuations is related to the intensity, dI, of the light scattered per unit solid angle $d\Omega$ by

$$\frac{I}{I_o}\frac{dI}{d\Omega} = \frac{k^4}{4\pi^2} < |\xi|^2 > f(\theta_o, \theta, N, \Delta)$$

$$= \frac{k^4}{4\pi^2}\left(\frac{k_B T}{\gamma q^2 + \Delta\rho g}\right) f(\theta_o, \theta, N, \Delta) \qquad (V.8)$$

where N is relative index of refraction of the scattering surface with respect to either air in the case of a surface or the other liquid in the case of an interface. The factor $f(\theta_o, \theta, N, \Delta)$, called the Fresnel coefficient of the interface is a purely geometric factor which has a value of $4(\cos\theta_o)^3$ for $\theta = \theta_o$ and $\Delta = 0$ [49]. The most important thing to note from Eq. V.8 is that $I \alpha q^{-2}$. This means that the surface waves are detectable even in the presence of scattering from bulk phonons.

The first experiments of this nature were performed by Vrij in 1964 [88]. They were however from self-supporting soap films and so will not be considered here.

Further to these experiments more classical light scattering experiments were performed by Lachaisse et al. [49] [50]. The experimental setup that they use is extremely complex with several optical elements and diaphrams [49]. This level of complication is needed for classical light scattering experiments due to the problem of the reflected beam interferring with the scattered light. This reflected beam (they call it parasitic light) must be reduced in order to have a good signal to noise ratio. For routine analysis this technique is too complicated to be useful. They were however able to apply it to a three phase system of 43.1% toluene, 49.5% brine, 4.95% sodium dodecyl sulfate and 2.45% butanol-1. They were able to determine the optical saturity which occurs when the middle phase has equal

parts brine and oil. At this point the interfacial tension is the same for both of the interfaces of the middle phase.

i) Quasi-elastic

Quasi-elastic light scattering (QELS) has been applied to various systems including free liquid surfaces, bilayers, films and interfaces. These will be dealt with separately in the section that follows. They all have the common quality however that it is necessary to know the dispersion relation, D(S), connecting the frequency of the ripplons to their wavelength. This in principle allows the determination of parameters such as ω_o the central frequency and Γ the width of the power spectrum, $P_q(\omega)$, of the scattered light which is the same as the power spectrum of the thermal ripplons [24]. ω_o is related to surface or interfacial tension and Γ is related to shear viscosity η. In specific cases it is also possible to obtain other parameters related to the surface.

All experiments regardless of the surface or interfacial systems unless otherwise indicated used experimental setups similar to the one illustrated in Figure 8. Earlier studies did not however employ the grating as a local oscillator for the heterodyne technique (to be described later) but used imperfections in the glass scattering cell.

a) Free Liquid Surface

The first light scattering experiments from a liquid surface were performed using a Fabry-Perot interferometer, as an extension of Brillouin scattering, by Katyl and Ingard in 1967 [47]. They proposed the existance of a Brillouin doublet in the case of underdamped waves but only spectral broadening from overdamped waves. They were able to correctly predict the ranges of density ρ and surface tension γ for which these two types of

scattering would occur from the dispersion relation,

$$D(S) = S^2 + 2S - (1 + 2S)^{1/2} + 1 + y = 0 \qquad (V.9)$$

where $$y = (\omega_o \tau_o)^2 \qquad (V.10)$$

$$\omega_o^2 = \frac{\gamma q^3}{\rho} \qquad (V.11)$$

$$\tau_o = \frac{1}{2\Gamma q^2} = \rho/2\eta q^2 \qquad (V.12)$$

and $$S = \alpha/2\Gamma q^2 \qquad (V.13)$$

where $\alpha = i\omega_o - \Gamma$.

There is no analytic solution to Equation V.9. Solving it numerically yields two roots which are complex conjugates for $y > 0.145$. This is manifested in damped oscillations and a Brillouin doublet. For $y < 0.145$, $Im(S) = 0$ and there are two modes, overdamped, which decay at different rates. They also note that the frequency separation of the two Brillouin peaks is $Im(S)/\pi\tau_o$ and the width of these peaks is $Re(S)/\pi\tau_o$. They performed experiments on two liquids, methanol and isopropanol, at $\Delta = 50^o$, $\theta = 70^o$ and $\theta_o = 80^o$. "y" has a value of 1.18 for methanol and 0.071 for isopropanol which spans well the ranges given above. They were not able to separate the doublet expected in methanol due to light scattered from below the surface which yielded a large background. They indicate however that it should be possible to eliminate this problem using heterodyne techniques. They also note that it is expected that to see the highest intensity of scattered light scattering must be detected close to the specularly

reflected beam. This is shown by Equation V.8 since $I \propto q^{-2}$. These same authors reported experiments the following year which employed the heterodyne technique and a spectrum analyzer to obtain $P_q(\omega)$ from the scattered light again in methanol [46]. They calibrated their apparatus in terms of $|\vec{q}|$, with artificially generated waves of a known wavelength. This calibration technique had been developed by them in another paper in 1968 [47]. They were able to observe the expected spectrum and verify that the theoretical dispersion equation, Equation V.9, was approximately correct. A review of this work appears in reference [45].

The theory and experiments of Katyl and Ingard were expanded by the group of Bouchiat and Meunier in three papers [9] [8] [61]. They chose the heterodyne technique and used imperfections in the glass scattering cell as a local oscillator. They again were able to verify the dispersion relation for ether (a damped system) and glycerine (an overdamped system). They also were able to perform some analysis to obtain the shear viscosity. The first two of these three papers show the possibilities for this method while the last gives more theoretical background and generates expressions for correlation functions, $G(\tau)$'s, and spectra, $P_q(\omega)$'s, for underdamped and overdamped cases. For overdamping ($y < 0.145$) the two solutions to Equation V.9 are real and negative (S_{1r} and S_{2r}) while for underdamping ($y > 0.145$) the solutions have negative real parts and are complex conjugates ($S_r \pm iS_i$). Using these facts they give the following expressions for $G(\tau)$ and $P_q(\omega)$ for these two cases.

For overdamping

$$G(\tau) = A\,[S_{2r}-S_{1r}]^{-1}[S_{2r}\exp(S_{1r}|\tau/\tau_o|)-S_{1r}\exp(S_{2r}|\tau/\tau_o|)] \quad (V.14)$$

$$P_q(\omega) = A \frac{2\, S_{2r} S_{1r}\, \tau_o}{S_{2r} - S_{1r}} \left[\frac{1}{\omega^2 \tau_o^2 + S_{1r}^2} - \frac{1}{\omega^2 \tau_o^2 + S_{2r}^2} \right] \qquad (V.15)$$

and for underdamping

$$G(\tau) = A \exp\left(S_r \left(\frac{\tau}{\tau_o}\right)\right) \left\{ \cos\left(S_i \left|\frac{\tau}{\tau_o}\right|\right) - \frac{S_r}{S_i} \sin\left(S_i \left|\frac{\tau}{\tau_o}\right|\right) \right\} \qquad (V.16)$$

$$P_q(\omega) = A \frac{S_r^2 + S_i^2}{S_i^2} \left\{ \frac{S_r}{S_r^2 + (\omega\tau_o + S_i)^2} + \frac{S_r}{S_i} \frac{(S_i + \omega\tau_o)}{\left[S_r^2 + (\omega\tau_o + S_i)^2\right]} \right\}$$

$$+ \frac{S_r}{S_i} \frac{S_i + \omega\tau_o}{\left[S_r^2 + (\omega\tau_o - S_i)^2\right]} + \frac{S_r}{S_i} \frac{S_i + \omega\tau_o}{\left[S_i^2 + (\omega\tau_o + S_i)^2\right]} \qquad (V.17)$$

where A is a constant.

The last two terms in Equation V.17 can not be neglected making it rather complicated. Of course in both cases $G(\tau)$ may be determined from $P_q(\omega)$ using the Wiener-Khintchine Theorem. In the overdamped case the $G(\tau)$ reduces to a sum of exponentials while in the case of underdamping $G(\tau)$ simplifies to a damped cosine function. This can be seen more easily if Equation V.13 is substituted into Equation V.16 yielding

$$G(\tau) = \text{constant} \exp(-\Gamma\tau) \cos(\omega_o \tau_o) \qquad (V.18)$$

An application of this technique to the liquid methoxy-benzilidine was performed by the Bouchiat-Meunier group in 1971 [6]. They found good agreement between experimental points and theoretical fits thus indicating the applicability of the classical dispersion equation (Equation V.9). Two

other papers by this group [7] [38] were basically reworkings of their previous publications with the second making the first comments on instrumental resolution, how it manifests itself and why it arises. They state that this finite resolution function broadens the observed spectrum and arises primarily from the fact that the incident laser beam covers more than one ripplon wavelength. It is of interest that they were able to obtain spectra with a laser as small as a 0.1 mW HeNe.

A review published by Langevin and Meunier in 1976 [53] sums up very well the work to that date. It includes two experimental details, one of which will be disputed later. These are; i) it is necessary to be very careful when approaching the critical point in a liquid since the scattering from the ripplons becomes very large and tends to overwhelm the local oscillator thus creating a homodyne signal for which the previous analysis does not apply, and ii) they state it is easier to examine the power spectrum of the scattered light than the correlation function. This will come into dispute at a later date when instrumental effects are included in the analysis.

The largest single improvement in experimental technique came in 1976 with the use of a transmission grating for the local oscillator as opposed to the imperfections in the glass scattering cell that were previously used [33]. The use of a grating provided two improvements. Firstly, the scattering angle and hence the scattering vector could now be calculated from the grating spacing "d" by using

$$q = \frac{2\pi n \cos \theta}{d} \qquad (V.18)$$

where "n" is the diffraction order. This also allows for the changing of

"q" quite easily by choosing differential diffraction orders. Secondly, large scale shaking was eliminated because the grating was shaking at the same frequency as the rest of the apparatus. These authors were able to determine the surface tension of water to about 2% and its viscosity to 10%. The exact specifications for gratings needed have been given by Edwards et al. [26].

In 1977, a paper by Stone and Rice [86] pointed out a greater problem with the state of the art in terms of surface tension determination using light scattering. They noted that better experiments were needed in order to properly evaluate the theories of capillary action present in the literature. This problem was addressed when improvements to the experiments were performed which introduced the addition of an instrumental resolution function to the data analysis [11]. Further improvements were made by this group again in 1985 [19]. They noted two facts regarding the form of the power spectrum of the light scattered by the ripplons. Firstly, the spectrum could very well be described by a Lorentzian and secondly, the inclusion of an instrumental term in the spectrum would require a convolution of the spectrum of the ripplons with this resolution function. The implications in terms of the correlation function are, i) it is roughly a damped cosine in shape and ii) this convolution is merely a product in the the time domain. Including these facts gives a correlation function of the form,

$$G(\tau) = A + B \cos(\omega_o \tau) \exp(-\Gamma\tau) \exp(\Delta^2\tau^2/4) \qquad (V.19)$$

where Δ is a fitted instrumental parameter and "A" and "B" are constants. They also noted that for $q < 2.70 \times 10^4 m^{-1}$ the β parameter, i.e. an

experimental resolution function is needed but not for larger q's. They were able to determine γ to 1% and η to 11% which was comparable to previous measurements by Hard [33]. They also indicate the advantages of using a grating. These authors published another paper in 1980 [10] which amplified their previous results and brought up the point that errors can arise in the determination of γ and η due to that lack of heterodyning. They also point out that it is important to determine that γ and η are independent of "q" in order to know that the experiments have been properly performed.

More recently a brief article has introduced a further level of complication into the problem [25]. This paper states that γ in fact might have a more complicated form, that is

$$\gamma(\omega) = \gamma_o + i\omega\eta_N \qquad (V.20)$$

where η_N is a normal viscosity component, γ_o is the static tension. A surface compressibility term, or elasticity, ξ, might also be of importance in the analysis. These are not however of interest for clean surfaces but will be examined more closely for monolayers and bilayers.

b) Surface and Self-Supporting Films

These systems will only be described briefly due to their limited applicability to oil/water interfaces. The initial experiments were performed on surface films in 1977 [32] [34]. These two experiments were of an entirely different nature in the sense that one group [32] used the older experimental methods without a diffraction grating and so had great difficulty determining the scattering vector. They also used an assumed rectangular instrumental function while the other group employed the grating technique and attemped more sophisticated modelling to determine film

elasticities and compressive and shear viscosities. This group also attempted to determine the film elasticity, ε, of a monomolecular propyl stearate film on water by using the equation

$$\varepsilon = A \frac{d\gamma}{dA} \qquad (V.21)$$

and changing the film area by using a moveable barrier. The first group did however use a light pipe to add some flexibility to the detection system and were able to show that the line widths they obtained were not due to convection but to real effects by changing the laser power and observing the line widths obtained.

These experiments were followed by experiments by Byrne and Earnshaw [12] and Langevin and Griesman [52] who studied fatty acid monolayers in order to determine elastic parameters. The second of these groups introduced a much more complicated dispersion relation into the problem.

The best paper in this area was produced in 1981 by Hard and Neuman [35]. They describe completely the experimental setup and data analysis techniques. They were able to examine films of lecithin and pentadecanvic acid on water in order to test the dispersion relation. This paper was followed closely by a paper by Langevin who studied films of propylstearatic, polyvinyl acetate, and polymethyl methacrylate on water.

A more recent paper by Crilly and Earnshaw [21] outlines more precisely the nature of the surface parameters that can be measured by light scattering and how they couple to the optical fields. They use monolayers of glycerol monooleate as an example system noting that the surface pressure, π, is defined as the increase in the surface tension due to the addition of a monolayer. That is

$$\pi = \gamma_s - \gamma \qquad (V.22)$$

where γ_s is the surface tension of the surface with a monolayer while γ is the surface tension of a clean surface. As well, they state that three of the four surface viscosity coefficients affect wave propagation with the surface shear viscosity being the only one which does not couple to the optical field. The two transverse shear viscosities, γ and η_N, perpendicular to the surface (as described by Equation V.19) and the dilation viscosity κ which is taken as a frequency dependent elasticity

$$\varepsilon = \varepsilon_o + i\omega\kappa \qquad (V.23)$$

do couple however. This is similar to the treatment of Hard and Lofgren [34]. Unfortunately, no analytic expression exists for η_N, γ, ε and κ as a function of the central frequency and width of the spectrum. As well, since these four parameters can not be obtained by fitting to two variables it is necessary to have some prior knowledge of the system. They constructed tables of ω_o (theoretical) and Γ (theoretical) for realistic values of η_N and κ using expressions given in the publication. The observed values of ω_o and Γ were the determined and the tables scanned. Of course, exact matches could only be found for a fine mesh of η_N and κ. This was unreasonable so the value of χ^2 was determined from

$$\chi^2 = \frac{[\omega_o - \omega_o \text{ (theoretical)}]^2}{V(\omega_o)} + \frac{[\Gamma - \Gamma(th)]^2}{V(\Gamma)} \qquad (V.24)$$

where $V(\omega_o)$ and $V(\Gamma)$ are the known variances of ω_o and Γ. This χ^2 was then interpolated to determine a best η_N and κ. It should be noted that for

fully compressed monolayers $\varepsilon = 0$. They also emphasize the need to perform experiments at different values of "q". This group again describes this technique in two papers in 1983 [24] [26]. The second of these describes very well the experimental setup and also the addition of a phase factor ϕ in the cosine term of Equation V.19 to account for the slightly non-Lorentzian nature of the spectrum. They also note that the largest errors in their measurements were due to motions and instabilities in the layers found. They also indicated that it is wise to average data sets at the same "a" and to plot the fit parameters as a function of "q" to get best results.

The last portion of this section will be a brief description of the light scattering technique as applied to self-supporting films. The first paper dealing with this subject was that of Fijnaut et al. [29]. A paper the next year showed experimentally the presence of a stretching mode in a film [44], with a subsequent paper by the same group [89] fully describing the theory of scattering by films. They note that there are correlation functions in the scattering from both bending and squeezing modes and that they may be combined to give an intermediate scattering function, $g^{(1)}(\tau)$ of

$$g^{(1)}(\tau) = \langle I_s(\tau)\rangle \exp[-\Gamma_s \tau] + \langle I_b(\tau)\rangle \exp(-\Gamma_b \tau)\cos(\omega_b \tau) \qquad \text{(V.25)}$$

where $g^{(1)}(\tau)$ is related to $G(\tau)$ by the Siegert relation

$$G(\tau) = A + B|g^{(1)}(\tau)|^2 \qquad \text{(V.26)}$$

and "b" and "s" refer to the bending and squeezing modes respectively and "A" and "B" are constants. They suggest using correlation analysis and fitting to a single exponential for studying the squeezing mode and spectrum analysis for studying the bending mode. Later papers by this group [42]

[43], give more detailed calculations and interpretations for scattering by films. They state in these papers that in general the bending mode is of more importance than the squeezing mode and depends on the thickness of the film and the surface tension.

c) Interfaces

The first paper in this area was in 1968 by Papoular [69]. He gave a full theoretical description of scattering from the interface between two infinite fluids. The next attempt at this area was not until 1980 when Pouchelon et al. performed experiments on the salt water:toluene:sodium dodecyl sulfate:butanol 1 system mixed in a ratio 49.95:46.35:1.95:3.75 by weight [72]. They simply used Equation V.8 for the expected intensity of the spectrum with $\Delta\rho$ being the difference in densities of the two fluids. They described the spectral width by

$$\Delta f = \frac{(\gamma+\Delta\rho g/q^2)q}{4\pi(\eta+\eta')} \qquad (V.27)$$

where η is the viscosity of the upper phase and η' is the viscosity of the lower. This same system in slightly different proportions was studied in 1981 by Chatenay et al. [17] who show the value of light scattering by pointing out it is particularly well suited to the study of interfaces due to the low interfacial tensions involved. These tensions may be lowered from 5×10^{-2} N/m to 10^{-6} N/m with the addition of a surfactant. They also note that by changing the salinity from 4% by weight to 10% by weight systems with an upper oil phase and a lower microemulsion phase may be changed to an upper oil phase, middle microemulsion phase, lower aqueous phase to an upper microemulsion, lower aqueous phase. These same techniques were later used by McLure and Pegg [63] Cazabat et al. [16] and Kim et al.

[48] on other systems.

The most complete and best paper on this particular system was published in 1984 by Lofgren et al. [54]. They performed measurements on the n-decane/water interface using the grating technique and an argon laser at about 150 mW of power. They did not measure the grating constant to determine the appropriate scattering vector but calculated the effective scattering vector by placing a mirror where the interface would be and noting that the wave vectors of surface waves that will scatter light into the detector will be given by

$$|\vec{q}| = \frac{2\pi \cos\theta}{\lambda} \frac{U}{R} \left(1 \pm \tan\left(\frac{\theta}{2}\right)\left(\frac{U}{R}\right)\right) \qquad (V.28)$$

where θ is as before, U is the distance between a chosen spot and the main beam and R is the distance between the interface and the detector plane. The distance U is measured using a travelling microscope on a photographic plate. This measurement can be made to a precision of about 0.2%. The uncertainty in R was about 0.6%. The effects of shrinkage of the image on developing is taken into account by moving the plate a known distance and taking a second exposure. They allowed their interfaces to equilibrate for about 24 hours before the date was taken. The correlation functions obtained were fit to an equation similar to Equation V.19, namely

$$G(\tau) = A + B \exp\left(-\Gamma\tau\left(1 - \frac{3}{8}\left(\frac{\Delta}{\Gamma}\right)^2\right)\right) \cos \omega_o \tau \qquad (V.29)$$

where β is the instrumental resolution. The parameters "A", "B", Γ, Δ and ω_o may be fit or Δ may be calculated approximately by

$$\Delta = \frac{0.6 \cos\theta\ \omega_o}{D\ q} \qquad (V.30)$$

where D is the beam width. They performed experiments at different values of "q" in order to verify the dispersion relation. The dispersion relation used by them was

$$\left[\eta_\omega(q + m_\omega) + \eta_d(q + m_d) - \frac{\varepsilon^* q^2}{i\omega} \right] \left[\frac{\eta_\omega \cdot m_\omega}{q}(q + m_w) + \frac{\eta_d \cdot m_d}{q}(q + m_d) \right.$$

$$\left. - \frac{\gamma q^2}{i\omega} \right] = \left[\eta_\omega(q - m_\omega) - \eta_d (q - m_d) \right]^2 \qquad \text{(V.31)}$$

where "ω" and "d" represent water and decane respectively and $m_j = [q^2 - (i\omega\rho_j/\eta_j)]^{1/2}$ for $j = \omega$ and d. ε is defined as in Equation V.23 and $\omega = \omega_o - i\alpha$ where α is the correction factor due to instrumental resolution from Equation V.28. For clean surfaces $\varepsilon_o = K = 0$ so $\varepsilon^* = 0$ and Equation V.30 may be solved for γ and η_d if η_ω, ρ_ω and ρ_d are known. Experiments at different values of "q" will then give γ and η_d. Problems in these measurements can arrive if the interface is tilted or curved since this distorts "q". It is also possible that heating of a coloured liquid might occur thus changing the γ measured. Care must be taken to have a clean system so as to avoid scattering from particulate contamination. These authors compared their results with determinations using the du Noüy ring, Wilhelmy plate and spinning drop. Table I shows a summary of those results.

Table 1

Interfacial Tensions at 20°C from Lofgren et al. [54]

Light Scattering	50.6 ± 0.6 Nm^{-1}
du Nouy Ring	52.0 ± 0.6 Nm^{-1}
Wilhelmy Plate	51.3 ± 0.6 Nm^{-1}
Spinning Drop	50.7 ± 0.7 Nm^{-1}

The agreement between techniques is quite good.

VII. Comparison of Light Scattering and Classical Techniques

Of the classical techniques examined previously, only three deserve serious consideration as methods to be used in the determination of interfacial tensions in oil/microemulsion systems. They are the pendant and sessile drop and spinning drop techniques. In the case of sessile drops, for low interfacial tensions (~ 10^{-6} Nm^{-1}), the technique of measuring the height of an infinitely large drop can produce a value of γ with an accuracy of 0.5% for a diameter to height ratio of about 4.8 [34]. This requires very careful measurement of the height and also that the assumptions that the contact angle is 180°, the thickness of the film between the drop and supporting glass and there is no error correction factor be met. If more realistic values of the precision of the drop height (~ 2%) measurement, and densities (~ 1%) are assumed overall errors of ~ 10% in γ are seen [23]. Errors between 1% and 10% appear to be the norm when these types of measurements are performed. More modern applications of the sessile drop technique which lend themselves to computerization, namely, digitizing the image of a sessile drop again generate errors in this range [81] [41] [13]. These last papers have the advantage that their methods are easily

applicable to both pendant and sessile drops.

Pendant drop measurements should in principle give approximately the same magnitude of errors since the same quantities are measured. There have however been some publications who claim errors in the fraction of percent range [71]. The advantages of the pendant drop method which also apply to sessile drop are as mentioned previously [2] i) a complete mathematical analysis is available ii) these techniques are independent of contact angle iii) no viscosity effects need to be taken into account iv) measurements can be made instantaneously v) successive measurements can be made on the same drop vi) low interfacial tensions can be measured ($0.4\ Nm^{-1} < \gamma < 3.0 \times 10^{-4}\ Nm^{-1}$) vii) any two transparent fluids can be used viii) small samples required ix) temperature control is possible and x) permanent photographic records are taken. Some exception may be taken to point i) in that solutions to Laplace's equation are not easy to obtain and fitting to it is even more difficult. The above statements were made when only approximations to the equation were available. An advantage that no authors mentioned is that these techniques are at least equilibrium in nature. Some of the disadvantages are i) very low vibration systems must be used ii) temperature control must be very good iii) if photos are used glass plates should be employed as opposed to paper due to differential shrinkage.

The spinning drop technique has a whole new range of problems associated with it due to the mechanical nature of the apparatus. Care must be taken to avoid vibration in the bearings and other moving parts and to use variable speed motors with a high degree of accuracy [83]. It is also necessary to have the apparatus very accurately in a horizontal position and to use elaborate illumination techniques if there is eccentricity in the

glass tube or in the axis of rotation. Having taken all of the above precautions it is still only possible to have a precision of about 2% if one waits for the order of 12 hours until the drop reaches a constant size. This technique is anything but equilibrium in nature.

Light scattering on the hand is equilibrium in nature and non-invasive. It does require a carefully controlled experimental setup in order to eliminate vibrations although heterodyne detection largely eleviates this problem. The errors that are seen are in the determination of γ in the same range as those for the spinning drop, du Noüy ring and Wilhelmy plate [54], roughly one or two percent. As in the case of the sessile drop, the mathematics of the technique has been largely worked out. Light scattering has several advantages, namely i) it may be applied to a large variety of systems from lipid bilayers [20] to oil/water systems [54], ii) as well as measuring γ to about 2%, the bulk phase shear viscosity may be measured [54], iii) it is non-invasive and only requires the knowledge of bulk properties and iv) with the proper exponential arrangement (as will be described in the last section) the same apparatus may be used to measure diffusion coefficients of micelles in the microemulsion phase.

Give all of the above advantages and the ease of computerized data collection and handling, light scattering appears to be a superior technique for measuring low interfacial tensions.

VII. Description of Light Scattering Apparatus

The proposed light scattering apparatus is based on the designs of Lofgren et al. [54] and Earnshaw [24] with modifications to allow for integration with the existing equipment at Energy, Mines and Resources (EMR)

at Devon. Figure 9a shows a top view of the arrangement. The dimensions given would allow the base-plate and scattering cell assembly to fit in the same position as the present scattering cell. The laser source need not be of great power as has been shown earlier but the existing argon laser could be utilized. The optical components consists basically of a lens, a transmission grating, a neutral density filter wheel and two beam director mirror systems. The grating may be custom made or purchased commercially however it is best to purchase the beam directors from a company such as Optikon. It might be necessary in the future to place a lens between the scattering cell and the detector. This can best be found out by experimentation. The only modification needed to the present E.M.R. system might be the shortening or elimination of the tube between the front and rear pinholes before the detector. Figure 9b shows a side view of the overall scattering system.

Figures 10a and 10b show the sample chamber from both a top view and side view. It has been designed to use standard 10 cm light path glass cuvettes of the type supplied by a compnay such as Hellma. This cell should probably be made from brass with the base plate made from aluminum. The large size of the cell allows for a great deal of heating or cooling field so as to supply adequate temperature regulation. This temperature regulation could be achieved by pumping in either warm or cold fluid or, if static heating is needed to reduce vibration, heating the cell with four soldering iron tips placed at positions 1 to 4. Regulation of the heating could take place using a controller such as those supplied by Omega.

The large slots for the entrance and exit of the laser beam allow for the acute incident angles needed for scattering from interfaces. The sides

of the cell have smaller slots for two reasons. Firstly, they allow for viewing of the sample interface in the case of interfacial tension measurement. Secondly, if the beam directors and grating are removed the cell may be used to perform diffusion coefficient measurements at scattering angles of 90° without disturbing the sample. This may be used to study the micellar phase of the emulsion.

Any standard autocorrelation may be used to analyze the scattered intensity fluctuations. The present E.M.R. system will suffice. Some software will have to be written to perform fits to Equation V.19 in order to obtain γ and η. This should probably be done using FORTRAN. Several non-linear least squares fitting algorithms are available to perform such fits.

Figure Captions

Figure 1 A diagram showing the geometry of a sessile drop.

Figure 2 A diagram showing the geometry of a pendant drop.

Figure 3 A block diagram of a spinning drop apparatus for determing interfacial tensions.

Figure 4 A diagram showing the geometry of a spinning drop.

Figure 5 A diagram showing the geometry of a flat meniscus.

Figure 6 The vertical tapered tube apparatus of Baird and Nirdosh [3].

Figure 7 The geometry of light scattering from a surface or interface.

Figure 8 A block diagram of the light scattering apparatus of Earnshaw [24].

Figure 9 A diagram of the proposed light scattering spectrometer.

Figure 10 A diagram of the proposed scattering chamber for scattering from interfaces and microemulsion regions.

Appendix I - Definition of Symbols

γ - Surface Tension (Nm^{-1})

g - Acceleration Due to Gravity (m/s^{-2})

ρ_1 - Density of More Dense Phase (kg/m^3)

ρ_2 - Density of Less Dense Phase (kg/m^3)

$\Delta\rho$ - Density Difference Between Two Phases ($\rho_1-\rho_2$) (kg/m^3)

Q - Angle Between Tangent to Meniscii and Horizontal Phase for Sessile and Pendant Drops

b - Radius of Curvature of Sessile or Pendant Drop at Apex (m)

β - Bashford and Adams Parameter ($\frac{\Delta\rho g b^2}{\gamma}$)

a - Capillary Constant ($\frac{2\gamma}{\Delta\rho g}$) (m)

Λ - Wave Length of Thermal Ripplons (m^{-1})

$\vec{q}$ - Wave Vector of Thermal Ripplons ($2\pi/\Lambda$) (m^{-1})

$\vec{K}$ - Scattering Vector for Radiation from Thermal Ripplons ($2\pi/\lambda$) (m^{-1})

λ - Wave Length of Radiation Incidention Surface or Interface (m)

ξ - Amplitude of Thermal Ripplons (m)

k_B - Boltzmann's Constant

T - Absolute Temperature (K)

η - Shear Viscosity ($kg\ s^{-1}\ m^{-1}$)

ν - Kinematic Viscosity (η/ρ) ($m^2\ s^{-1}$)

References

[1] Adamson, A.W., Physical Chemistry of Surfaces, New York, Interscience Publishers, 1960.

[2] Andreas, J.M., E.A. Hauser and W.B. Tucker, 1938. Boundary tension by pendant drops. J. Phys. Chem. 42, 1001-1019.

[3] Baird, M.H.I. and I. Nirdosh, 1981. Surface and interfacial tension measurement by drainage methods. Can. J. Chem. Eng. 59, 369-376.

[4] Bashford, F. and J.C. Adams. An Attempt to Test Theories of Capillary Action. University Press. Cambridge, 1883.

[5] Baus, M., 1982. Elastic moduli of a liquid-vapour interface. J. Chem. Phys. 76, 2003-2009.

[6] Bouchiat, M.A. et D. Langevin, 1971. Comparison entre le spectre expérimental et le spectre théoretique de la lumière diffusée par la surface libre d'un liquide simple. C.R. Acad. Sc. Paris 272B, 1357-1359.

[7] Bouchiat, M.A. et J. Meunier, 1971. Spectre des fluctuations thermiques de la surface libre d'un liquide simple. J. de Physique. 32, 561-571.

[8] Bouchiat, M.A. et J. Meunier, 1968. Caractéristiques du spectre de la lumière diffusée par les ondes de capillarité présentes sur la surface d'un liquide. C.R. Acad. Sc. Paris 266B, 301-304.

[9] Bouchiat, M.A., J. Meunier et J. Brossel, 1968. Mise en évidence des ondes de capillarité excitées thermiquement à la surface d'un liquide par diffusion inélastique de lumière cohérente. C.R. Acad. Sc. Paris 266B, 255-258.

[10] Byrne, D. and J.C. Earnshaw, 1980. Experimental tests of theories of capillary wave propagation. J. Coll. Int. Sc. 74, 467-473.

[11] Byrne, D. and J.C. Earnshaw, 1979. Photon correlation spectroscopy of liquid interfaces: I. Liquid-air interfaces. J. Phys. D.: Appl. Phys. 12 1133-1144.

[12] Byrne, D. and J.C. Earnshaw, 1979. Photon correlation spectroscopy of liquid interfaces: II. Monolayers of fatty acids. J. Phys. D.: Appl. Phys. 12, 1145-1157.

[13] Boyce, J.F., S. Schurch, Y. Rotenberg and A.W. Neumann, 1984. The measurement of surface and interfacial tension by the axisymmetric drop technique. Colloids and Surfaces. 9, 307-317.

[14] Butler, J.N. and B.H. Bloom, 1966. A curve-fitting method for calculating interfacial tension from the shape of a sessile drop. Surface Sci. 4, 1-17.

[15] Cayias, J.L., R.S. Schechter and W.H. Wade. The measurement of low interfacial tension via the spinning drop technique. In Adsorption at Interfaces. Ed. K.L. Mittal, Washington, D.C., American Chemical Society, 1975, p. 234-247.

[16] Cazabat, A.M., D. Langevin, J. Meunier and A. Pouchelon, 1982. Critical behaviour in microemulsions. Adv. Coll. Int. Sci. 16, 175-199.

[17] Chatenay, D., D. Langevin, J. Meunier and A. Pouchelon. Light scattering by oil-water interfaces. In Scattering Techniques Applied to Supramolecular and Nonequilibrium Systems. Ed. S.-H. Chen, B. Chu and R. Nossal. New York. Plenum Pres. 1981, p. 795-801.

[18] Coucoulas, L.M. and R. Dawe, 1985. The calculation of interfacial tension from sessile drops. J. Coll. Int. Sci. 103, 230-236.

[19] Crilly, J.F. and J.C. Earnshaw, 1985. Light scattering from fluid interfaces: considerations of some instrumental effects. J. Phys. D: Appl. Phys. 18 609-616.

[20] Crilly, J.F. and J.C. Earnshaw, 1983. Photon correlation spectroscopy of bilayer lipid membranes. Biophys. J. 41, 197-210.

[21] Crilly, J.F. and J.C. Earnshaw. The surface viscosity of fully condensed monolayers of glycerol monooleate. In Biomedical Applications of Laser Light Scattering. Ed. D.B. Sattelle, W.I. Lee and B.R. Ware. Amsterdam, Elsevier Biomedical Press., 1982. Pp 123-135.

[22] Dismukes, E.B., 1959. The effect of drop size on the accuracy of surface tension determinations by the sessile drop method. J. Phys. Chem. 63, 312-314.

[23] Dunlap-Wilson, P.M. and C.F. Brandner, 1977. Aqueous surfactant solutions which exhibit ultra-low tensions at the oil-water interface. J. Coll. Int. Sci. 60, 473-479.

[24] Earnshaw, J.C. Light scattering by model membranes. In the Application of Laser Light Scattering to the Study of Biological Motion. Ed. J.C. Earnshaw and M.W. Steer, New York, Plenum Press, 1983. Pp 274-299.

[25] Earnshaw, J.C., 1981. Surface viscosity of water. Nature 292, 138-139.

[26] Edwards, R.V., R.S. Sirohi, J.A. Mann, L.B. Shih and L. Lading, 1982. Surface fluctuation scattering using grating heterodyne spectroscopy. Appl. Opt. 21, 3555-3568.

[27] Faetti, S. and V. Palleschi, 1984. Measurements of the interfacial tension between nematic and isotropic phase of some cyanobiphanyls. J. Chem. Phys. 81, 6254-6258.

[28] Fieber, C. and H. Sonntag, 1979. Theoretical considerations on the applicability of the sphere method for measuring interfacial tension and contact angle. Coll. Polymer Sci. 257, 874-881.

[29] Fijnaut, H.M. and J.G.H. Joosten, 1978. Relaxation of the squeezing mode in free liquid films, measured by laser light scattering. J. Chem. Phys. 69, 1022-1029.

[30] Girault, H.H.J., D.J. Schriffrin and B.D.V. Smith, 1984. The measurement of interfacial tension of pendant drops using a video image profile digitizer. J. Coll. Int. Sci. 101, 257-266.

[31] Girault, H.H., D.J. Schriffrin and B.D.V. Smith, 1982. Drop image processing for surface and interfacial tension measurements. J. Electroanal. Chem. 137, 207-217.

[32] Grabowski, E.F. and J.A. Cowen, 1977. Thermal excitations of a bilipid membrane. Biophys. J. 18, 23-28.

[33] Hard, S., Y. Hamnerius and O. Nilsson, 1976. Laser heterodyne apparatus for measurements of liquid surface properties - Theory and experiments. J. Appl. Phys. 47, 2433-2442.

[34] Hard, S. and H. Lofgren, 1977. Elasticity and viscosity measurements of monomolecular propyl stearate films at air-water interfaces using laser light scattering techniques. J. Coll. Int. Sci. 60, 529-539.

[35] Hard, S. and R.D. Neuman, 1981. Laser light-scattering measurements of viscoelastic monomolecular films. J. Coll. Int. Sci. 83, 315-334.

[36] Healy, R.N. and R.L. Reed, 1974. Physiochemical aspects of microemulsion flooding. Soc. Pet. Eng. J. 14, 491-501.

[37] Healy, R.N., R.L. Reed and D.G. Stenmark, 1976. Multiphase microemulsion systems. Soc. Pet. Eng. J., June, 147-160.

[38] Herpin, J.C. et J. Meunier, 1974. Étude spectrale de la lumière diffusée par les fluctuations thermiques de l'interface liquide vapeur de CO_2 près de son point critique. Mesure de la tension superficielle et de la viscosité. J. de Physique 35, 847-859.

[39] Huh, C. and S.G. Mason, 1976. Sphere tensiometry: an evaluation and critique. Can. J. Chem. 54, 969-978.

[40] Huh, C. and S.G. Mason, 1975. A rigorous theory of ring tensiometry. Colloid and Polymer Sci. 253, 566-580.

[41] Huh, C. and R.L. Reed, 1983. A method for estimating interfacial tensions and contact angles from sessile and pendant drop shapes. J. Coll. Int. Sci. 91, 472-484.

[42] Joosten, J.G.H., 1984. Spectral analysis of light scattered by liquid films. I. General considerations. J. Chem. Phys. 80, 2363-2382.

[43] Joosten, J.G.H., 1984. Spectral analysis of light scattering by liquid films. II. Light scattering in the long wavelength limit. J. Chem. Phys. 80, 2383-2400.

[44] Joosten, J.G.H. and H.M. Fijnaut, 1979. Detection of the relaxation of the stretching mode in thin liquid films. Chem. Phys. Lett. 60, 483-485.

[45] Katyl, R.H. and U. Ingard. Light scattering from thermal fluctuations of a liquid surface. In Honor of Philip M. Morse. Ed. H. Feshback and K.U. Ingard. Cambridge, MA. The M.I.T. Press, 1969, p. 70-87.

[46] Katyl, R.H. and U. Ingard, 1968. Scattering of light by thermal ripplons. Phys. Rev. Lett. 20, 248-249.

[47] Katyl, R.H. and U. Ingard, 1967. Line broadening of light scattered from a liquid surface. Phys. Rev. Lett. 19, 64-66.

[48] Kim, M.W., J. Bock and J.S. Huang. Interfacial and critical phenomena in microemulsions. In Waves on Fluid Interfaces. Ed. R.E. Meyer. New York, Academic Press, 1983, p. 151-165.

[49] Lachaise, J., A. Graciaa, A. Martinez and A. Rousset, 1979. Measurement of low interfacial tensions from the intensity of the light scattered by liquid interfaces. J. Physique Lett. 40, L599-L602.

[50] Lachaise, J., A. Graciaa, A. Martinez et A. Rousset, 1979. Mesure de faibles tensions interfacial à partir de l'intensité de la lumière diffusée par des interfaces liquides. C.R. Acad. Sc. Paris. 289B, 73-77.

[51] Langevin, D, 1981. Light scattering study of monolayer viscoelasticity. J. Coll. Int. Sci. 80, 412-425.

[52] Langevin, D. and C. Griesmar, 1980. Light scattering study of fatty acid monolayers. J. Phys. D: Appl. Phys. 13, 1189-1199.

[53] Langevin, D. and J. Meunier. Light scattering by liquid interfaces in Photon Correlation Spectroscopy and Velocimetry. Ed. H.Z. Cummins and E.R. Pike, New York, Plenum Press, 1976, p. 501-518.

[54] Lofgren, H., R.D. Neuman, L.E. Scriven and H.T. Davis, 1984. Laser light scattering measurements of interfacial tensions using optical heterodyne mixing spectroscopy. J. Coll. Int. Sci. 98, 175-183.

[55] Los, J.M. H. Vos and J. Wagenaar, 1978. Striascopic imaging of reflected profiles with laser light and the interfacial tension of fluid interfaces. J. Phys. E: Sci. Instrum. 11, 1027-1032.

[56] Malcolm, J.D. and C.D. Elliott, 1980. Interfacial tension from height and diameter of a single sessile drop or captive bubble. Can. J. Chem. Eng. 58, 151-153.

[57] Malcolm, J.D. and H.M. Paynter, 1981. Simultaneous contact angle and interfacial tension from sessile drop measurements. J. Coll. Int. Sci. 82, 269-275.

[58] Manning, C.D. and L.E. Scriven, 1977. On interfacial tension measurement with a spinning drop in gyrostatic equilibrium. Rev. Sci. Instrum. 48, 1699-1705.

[59] Maze, C. and G. Burnett, 1971. Modifications of a non-linear regression technique used to calculate surface tension from sessile drops. Surface Sci. 24, 335-342.

[60] Maze, C. and G. Burnett, 1969. A non-linear regression method for calculating surface tension and contact angle from the shape of a sessile drop. Surface Sci. 13, 451-470.

[61] Meunier, J., D. Cruchon et M.A. Bouchiat, 1969. Etude expérimentale des ondes de capillarité excitées thermiquement à la surface d'un liquide pur pour les régimes hydrodynamiques proches de l'amortissement critique. C.R. Acad. Sc. Paris. 268B, 422-425.

[62] Michaels, A.S. and E.A. Hauser, 1951. Interfacial tension at elevated pressure and temperature. II. J. Phys. Chem. 55, 408-421.

[63] McLure, I.A. and I.L. Pegg, 1982. Laser light scattering spectroscopy on thermally excited capillary waves at liquid-liquid interfaces in binary liquid mixtures near critical end-points. J. Mol. Struct. 80, 393-400.

[64] Needham, D. and D.A. Haydon, 1983. Tensions and free energies of formation of "solventless" lipid bilayers. Measurement of high contact angles. Biophys. J. 41, 251-257.

[65] Oh, S.G. and J.C. Slattery, 1979. Interfacial tension required for significant displacement of residual oil. Soc. Pet. Eng. J. 19, 83-96.

[66] Padday, J.F., 1972. Sessile drop profiles: corrected methods for surface tension and spreading coefficients. Proc. R. Soc. Lond. A 330, 561-572.

[67] Padday, J.F. and A.R. Pitt, 1972. Surface and interfacial tensions from the profile of a sessile drop. Proc. R. Soc. Lond. A 329, 421-431.

[68] Padday, J.F., 1971. The profiles of axially symmetric meniscii. Phil. Trans. Roy. Soc. Lond. A 269, 265-293.

[69] Papoular, M., 1968. Ondes de surface dans un système de deux phases fluides superposées. J. de Physique 29, 81-87.

[70] Patterson, H.T., K.H. Hu and T.H. Grindstaff, 1971. Measurement of interfacial and surface tensions in polymer systems. J. Polymer Sci: Part C 34, 31-43.

[71] Patterson, R.E. and S. Ross, 1979. The pendent-drop method to determine surface or interfacial tensions. Surface Sci. 81, 451-463.

[72] Pouchelon, A., J. Meunier, D. Langevin and A.M. Cazabat, 1980. Light scattering from oil-water interfaces: measurements of low interfacial tensions. J. Physique Lett. 41, L239-L242.

[73] Princen, H.M., I.Y.Z. Zia and S.G. Mason, 1967. Measurement of interfacial tension from the shape of a rotating drop. J. Coll. Int. Sci. 23, 99-107.

[74] Puig, J.E., E.I. Franses, H.T. Davis, W.G. Miller and L.E. Scriven, 1979. On interfacial tensions measured with alkyl aryl sulfonate surfactants. Soc. Pet. Eng. J. 19, 71-82.

[75] Qutubuddin, S., C.A. Miller and T. Fort, 1984. Phase behavior of pH-dependent microemulsions. J. Coll. Int. Sci. 101, 46-58.

[76] Rama Rao, N.V. and M.H.I. Baird, 1983. A simple technique for the measurement of surface and interfacial tension. J. Phys. E: Sci. Instrum. 16, 1164-1166.

[77] Rao, N.V.R. and M.H.I. Baird, 1983. Continuous measurement of surface and interfacial tension by stationary slug method. Can. J. Chem. Eng. 61, 581-589.

[78] Rewick, R.T., K.A. Sabo and J.H. Smith, 1982. A dispersant effectiveness test based on the drop-weight interfacial test method. J. Test. Eval. 10, 72-74.

[79] Rosano, M.L., D. Jon and J.H. Whittam, 1982. Considerations on formation and solubility of oil/water dispersed systems. J. Am. Oil Chem. Soc. 59, 360-363.

[80] Rosenthal, D.K., 1962. The shape and stability of a bubble at the axis of a rotating liquid. J. Fluid Mech. 12, 358-366.

[81] Rotenberg, Y., L. Boruvka and A.W. Neumann, 1983. Determination of surface tension and contact angle from the shapes of axisymmetric fluid interfaces. J. Coll. Int. Sci. 93, 169-183.

[82] Seeto, Y., J.E. Puig, L.E. Scriven and H.T. Davis, 1985. Interfacial tensions in systems of three liquid phases. J. Coll. Int. Sci. 96, 360-372.

[83] Seeto, Y. and L.E. Scriven, 1982. Precision spinning drop interfacial tensiometer. Rev. Sci. Instrum. 53, 1757-1761.

[84] Staicopolus, D.N., 1962. The computation of surface tension and of contact angle by the sessile drop method. J. Coll. Sci. 17, 439-447.

[85] Stauffer, C.E., 1965. The measurement of surface tension by the pendant drop technique. J. Phys. Chem. 69, 1933-1938.

[86] Stone, J.A. and W.J. Rice, 1977. Adequacy of several theories of capillary wave damping for drawing inferences of the interfacial properties of gas-liquid interfaces. J. Coll. Int. Sci. 61, 160-169.

[87] Qutubuddin, S., C.A. Miller and T. Fort, 1984. Phase behavior of pH-dependent microemulsions. J. Coll. Int. Sci. 101, 46-58.

[88] Vrij, A., 1964. Light scattering by soap films. J. Coll. Sci. 19, 1-27.

[89] Vrij, A., G.H. Joosten and H.M. Fijnaut. Light scattering from thin liquid films. In Advances in Chemical Physics Vo. XLVIII. Ed. I. Prigogine and S.A. Rice, New York, Interscience Publishers. 1981. P330-392.

[90] Warren, C. and W.W. Webb, 1969. Interfacial tension of near-critical cyclohexane-methanol mixtures. J. Chem. Phys. 50, 3694-3700.

[91] Wielinski, D. and G.H. Findenegg, 1984. Measurement of interfacial tension in simple two-phase ternary systems along an isothermal linear path to the critical point. J. Phys. Chem. 88, 4397-4401.

[92] Wims, A.M., J.V. Sengers, D. McIntyre and J. Shereshefsky, 1970. Interfacial tension of 3-methylpentane-nitroethane near the critical point. J. Chem. Phys. 52, 3042-3049.

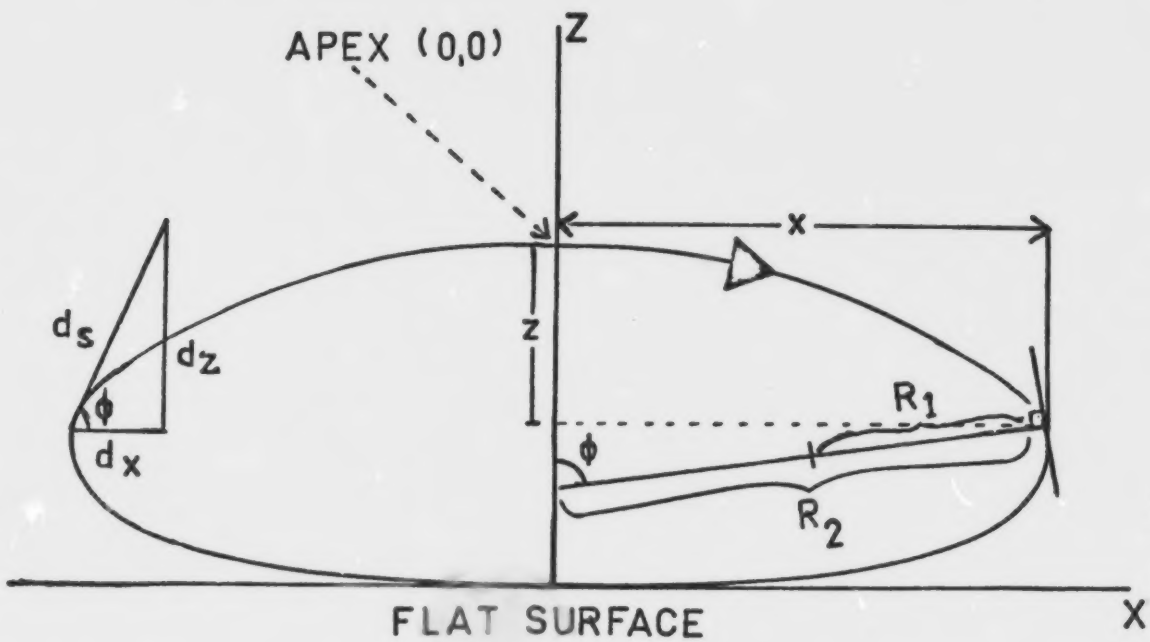
APEX (0,0)
Z
x
z
d_s
d_z
d_x
ϕ
R_1
R_2
FLAT SURFACE
X

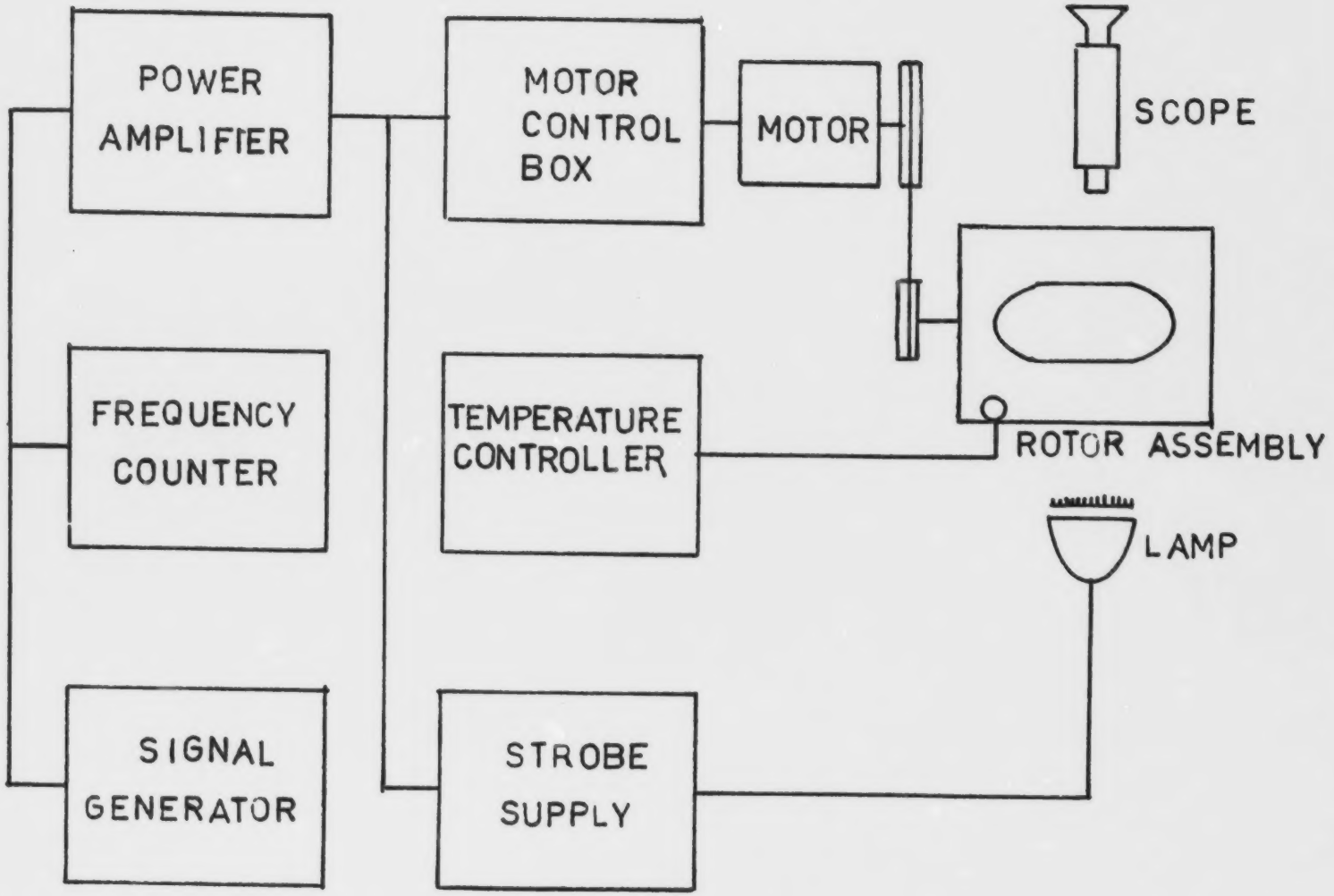
POWER AMPLIFIER
MOTOR CONTROL BOX
MOTOR
SCOPE
FREQUENCY COUNTER
TEMPERATURE CONTROLLER
ROTOR ASSEMBLY
LAMP
SIGNAL GENERATOR
STROBE SUPPLY

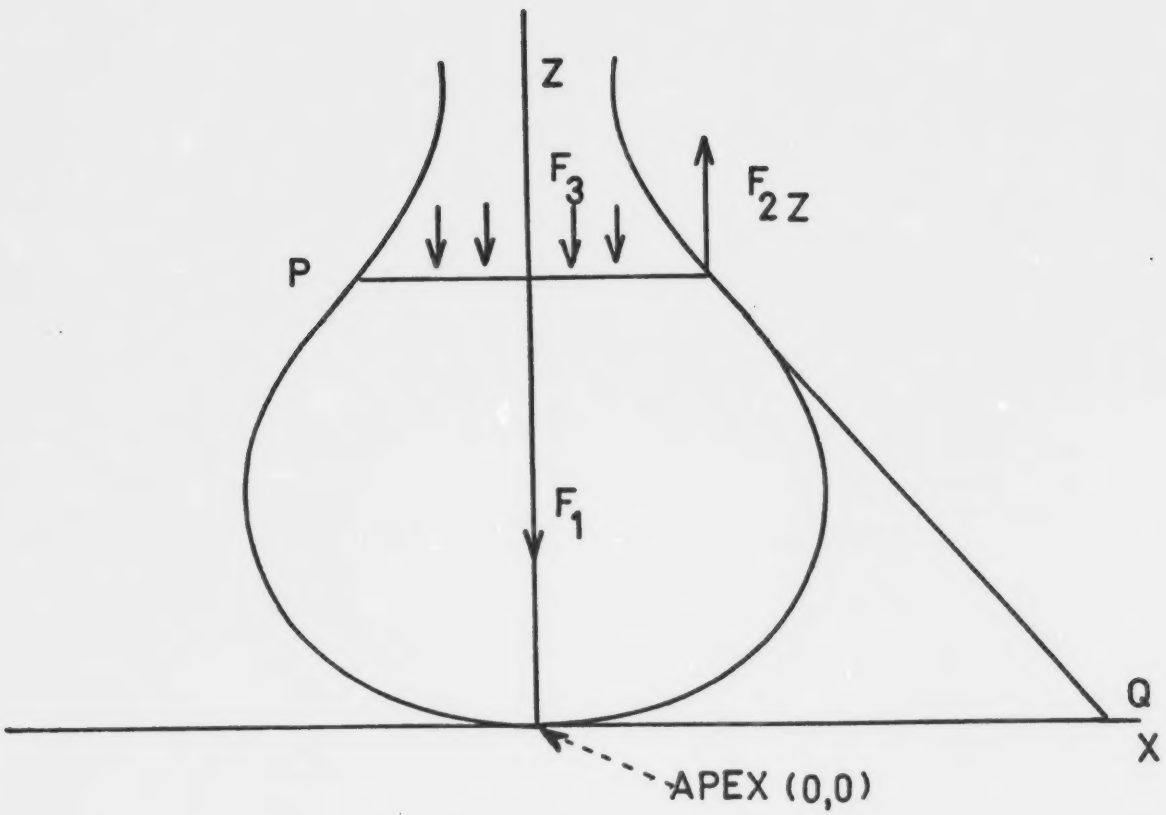
Z
F3
F2Z
P
F1
Q
X
APEX (0,0)

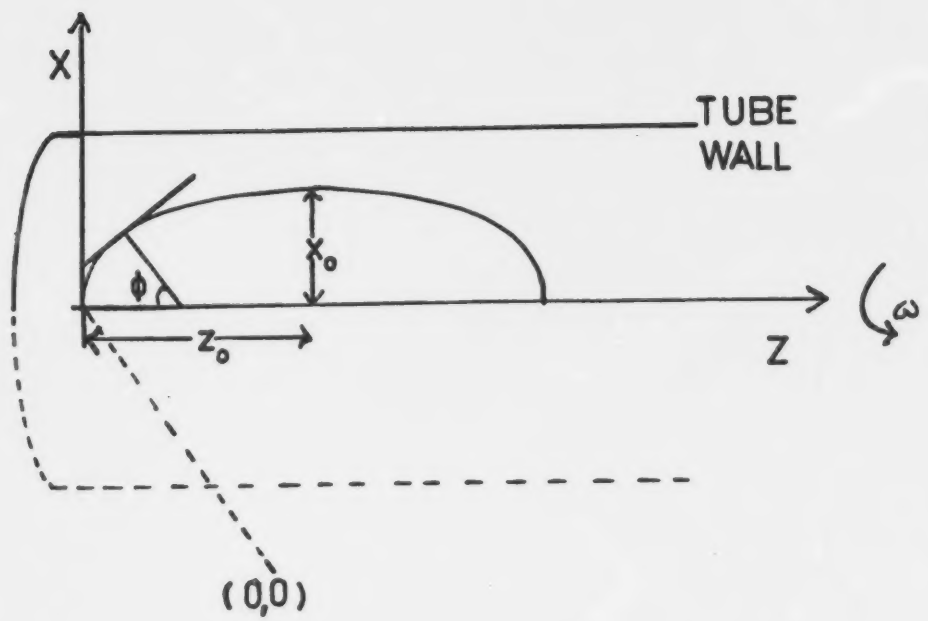
X
TUBE
WALL
X_o
ϕ
Z_o
Z
ω
(0,0)

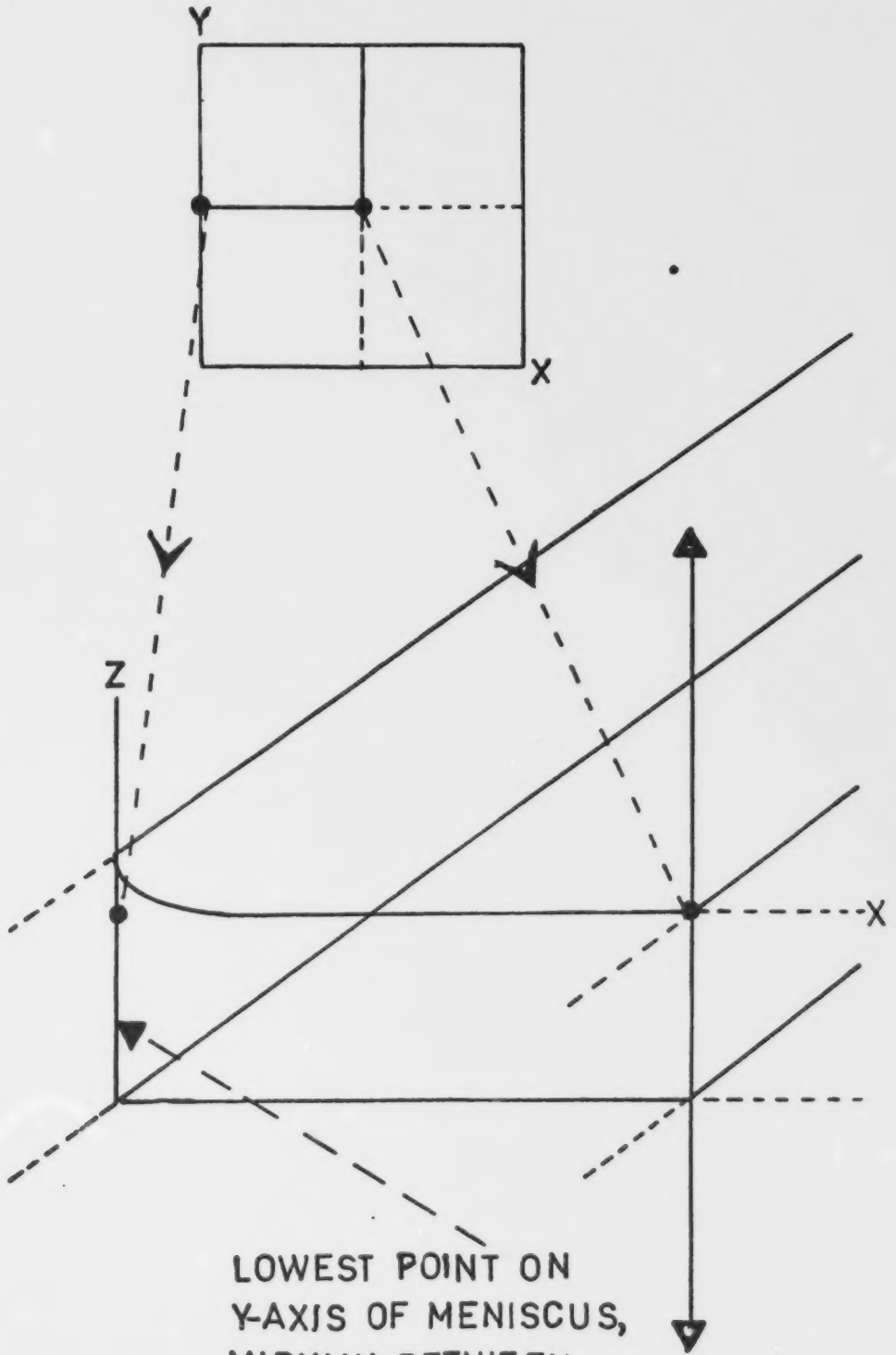
Y
X
Z
X
LOWEST POINT ON
Y-AXIS OF MENISCUS,
MIDWAY BETWEEN
WALLS.

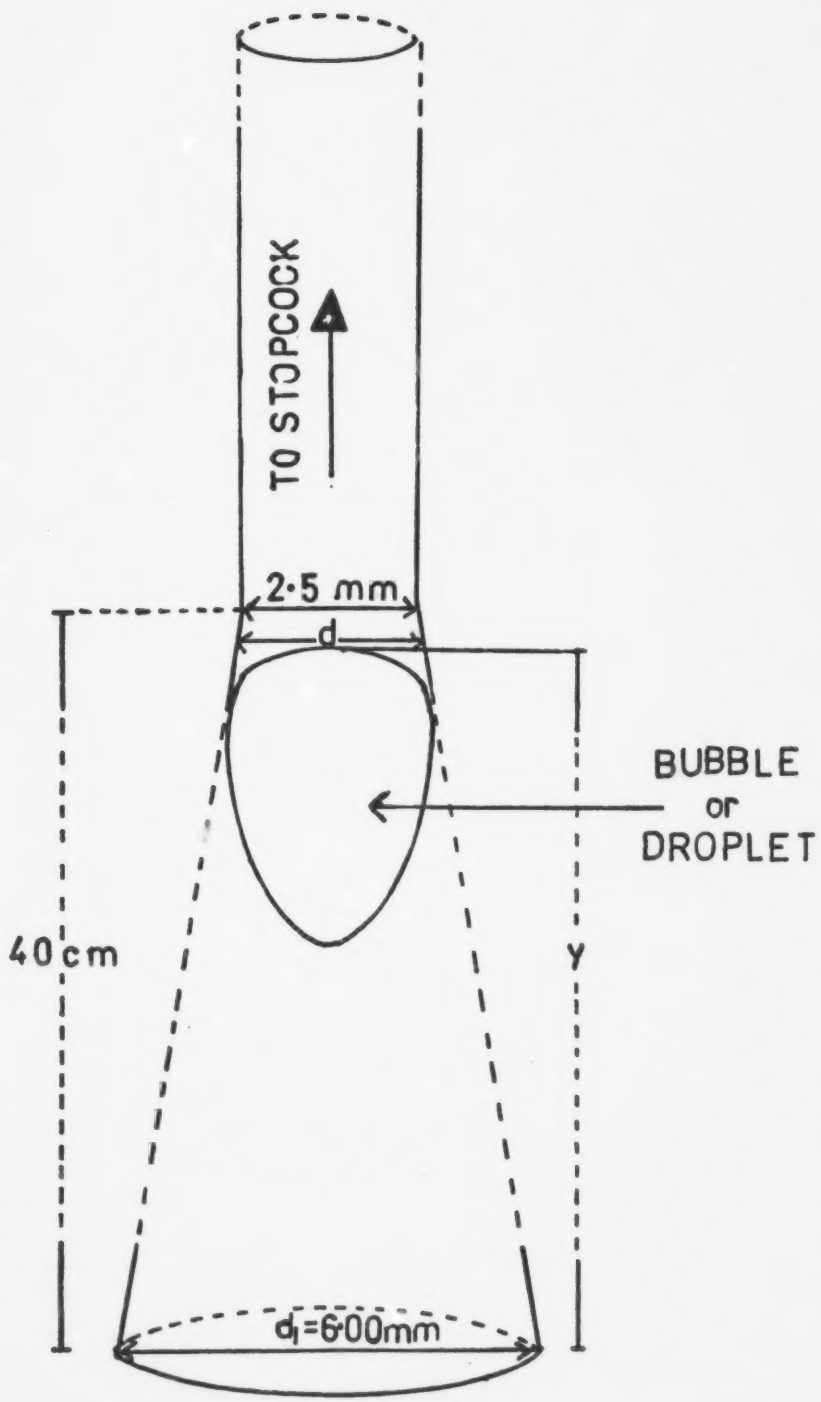
TO STOPCOCK
2·5 mm
d
BUBBLE
or
DROPLET
40 cm
y
d_1=6·00mm

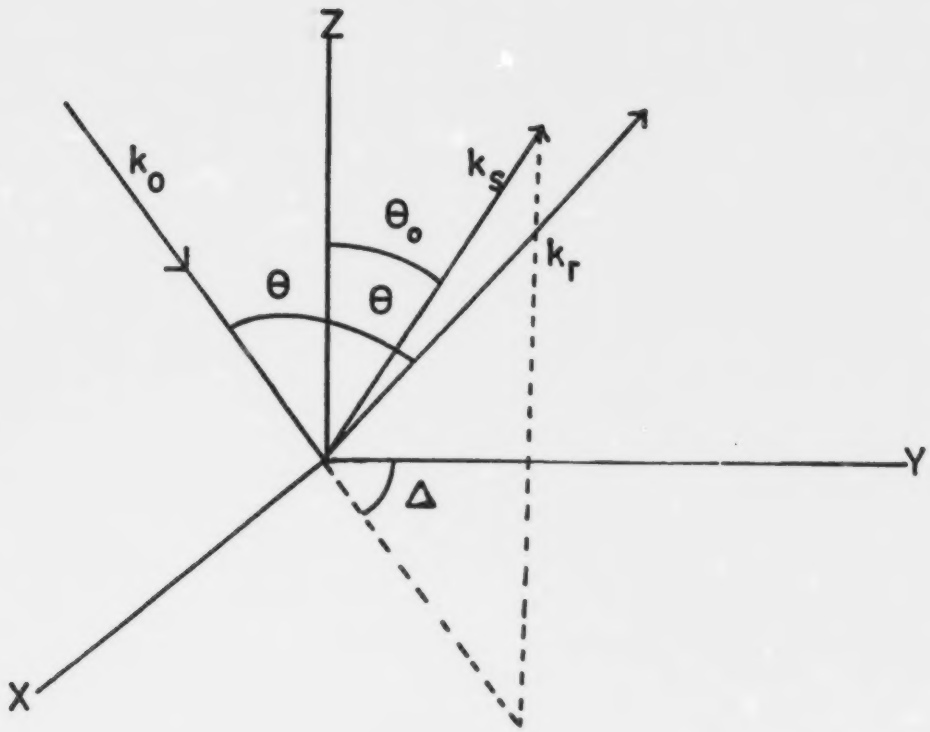
Z
k_o
k_s
θ_o
k_r
θ
θ
Y
Δ
X

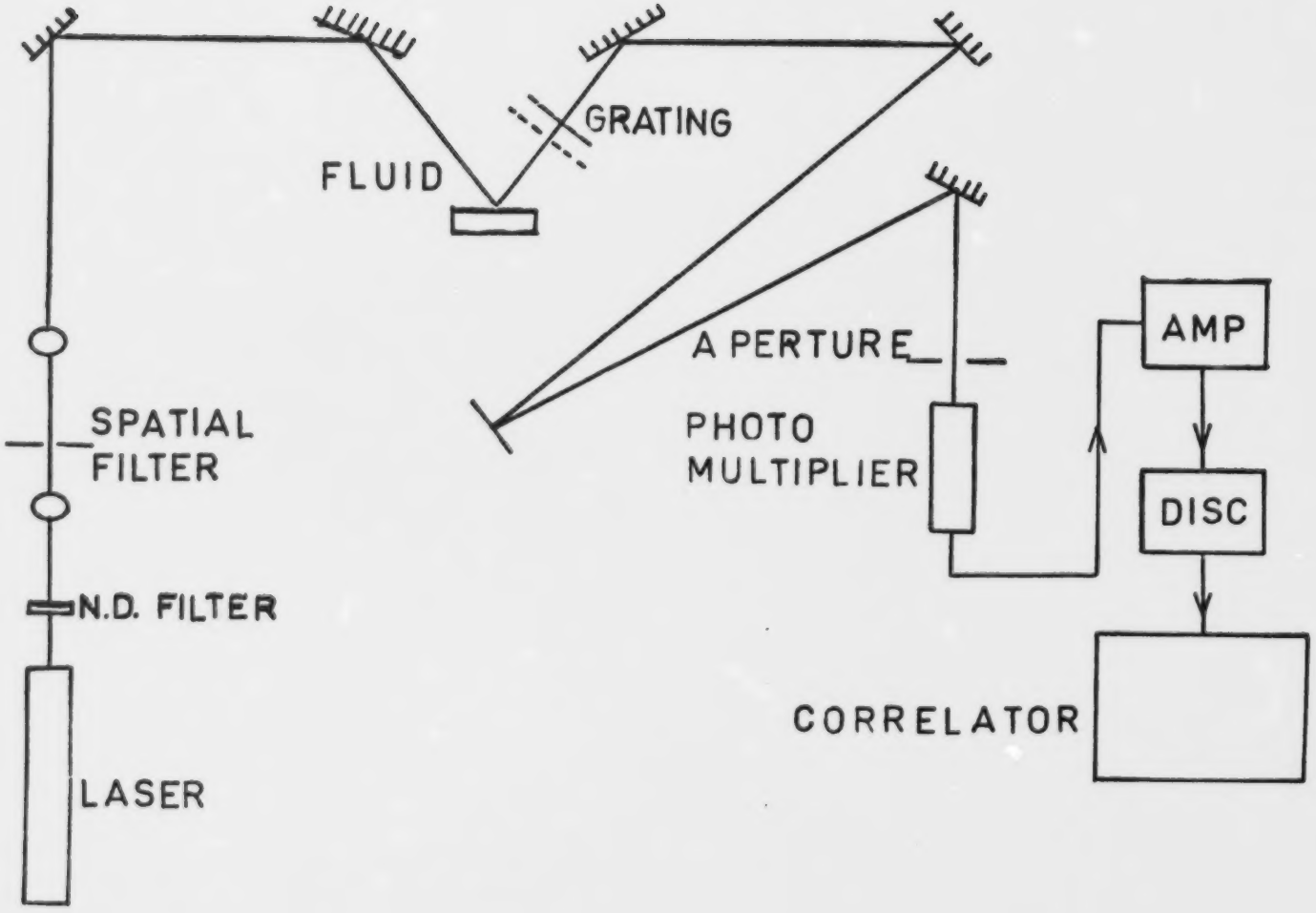
GRATING
FLUID
APERTURE
AMP
SPATIAL
FILTER
PHOTO
MULTIPLIER
DISC
N.D. FILTER
CORRELATOR
LASER

TOP VIEW

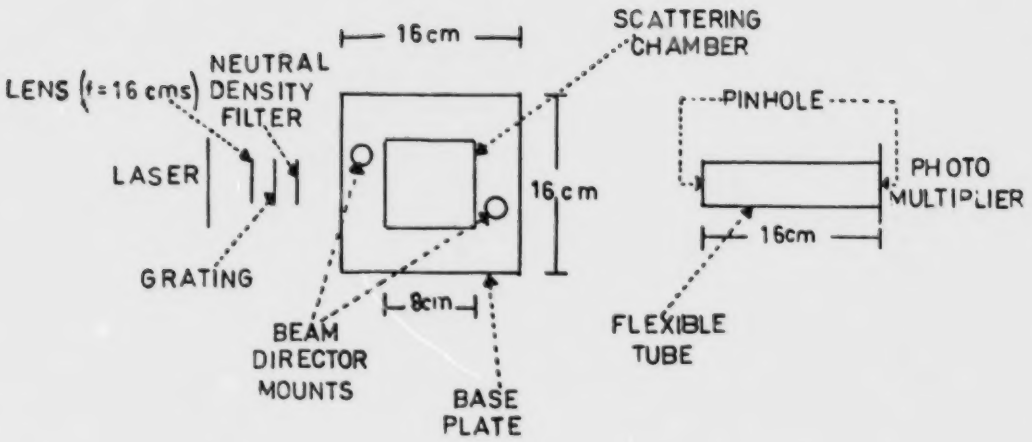

SIDE VIEW

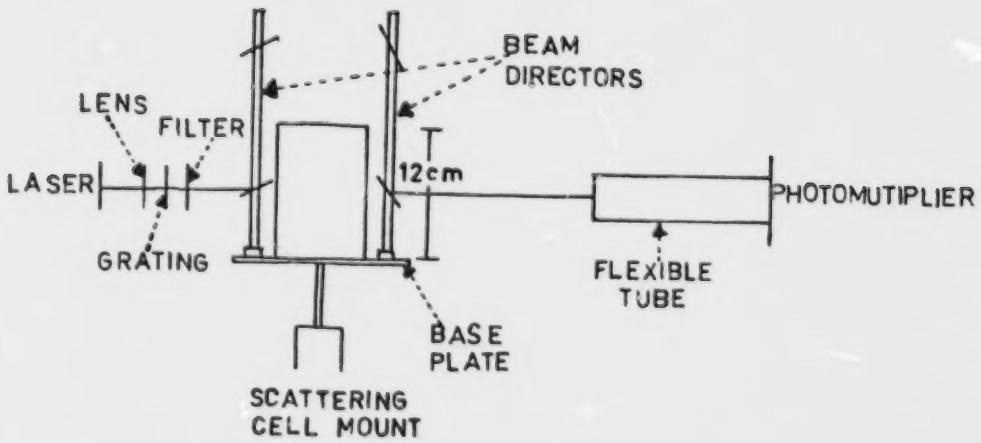

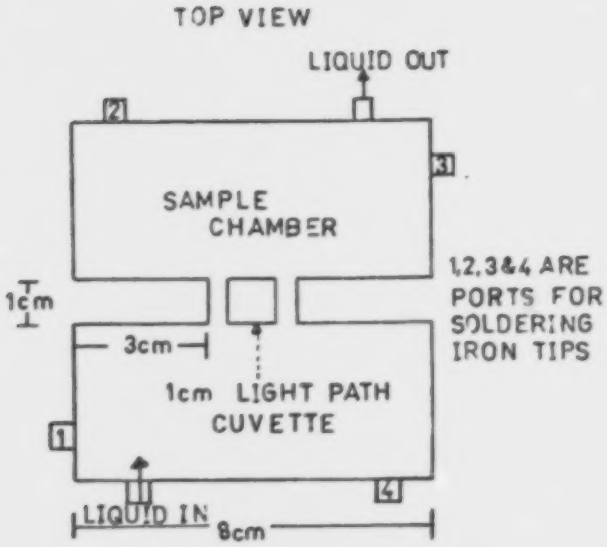
TOP VIEW
LIQUID OUT
2
3
SAMPLE CHAMBER
1,2,3&4 ARE PORTS FOR SOLDERING IRON TIPS
1cm
3cm
1cm LIGHT PATH CUVETTE
1
4
LIQUID IN
8cm

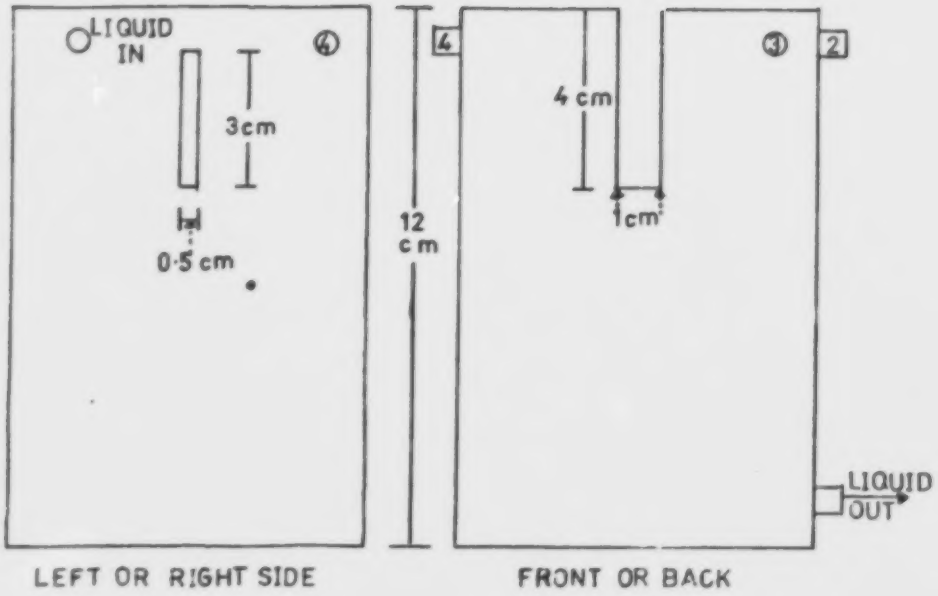
LIQUID IN
4
3cm
0·5 cm
12 cm
4
3
2
4 cm
1cm
LIQUID OUT
LEFT OR RIGHT SIDE
FRONT OR BACK